Aeronomy and astrophysics

Palmer Station measurements of radio atmospherics associated with upward electrodynamic coupling phenomena between thunderstorms and the mesosphere/lower ionosphere

S.C. REISING, U.S. INAN, *and* T.F. BELL, *Space, Telecommunications, and Radioscience Laboratory, Stanford University, Stanford, California 94305*

The past several years have produced an unusual surge of new scientific evidence indicating strong electrodynamic coupling between phenomena occurring in regions of tropospheric thunderstorms, at altitudes below 10–15 kilometers (km), and the mesosphere/lower ionosphere, ranging in altitude up to 100 km. Prominent examples of this coupling are the optical flashes in the mesosphere known as "sprites," "jets," and "elves." Measurements from aircraft (Sentman et al. 1995) and from the ground (Lyons 1994) show that sprites appear at altitudes from approximately 50 km to approximately 90 km, are red in color, and last for tens of milliseconds (ms). Blue jets expand upward from the cloud tops to approximately 50 km altitude, last for as long as 100 ms, and disappear all at once (Wescott et al. 1995). Elves are typically observed over a 500–600-km-wide region, in the 80- to 95-km altitude range, just above where most sprites occur (Inan et al. 1997). Elves expand outward from their center point, directly above the causative lightning flash, and are over in less than 1 ms.

While the optical measurements and very-low-frequency (VLF) remote sensing of associated ionospheric disturbances (i.e., early/fast VLF events) (Inan, Rodriguez, and Idone 1993) are conducted in the Northern Hemisphere, ongoing broadband VLF observations at Palmer Station have proven to be extremely useful in identification of features of the causative lightning discharges that lead to these newly realized electrodynamic coupling effects. In this connection, it is important to note that the low background radio noise levels at Palmer Station provide a unique opportunity to monitor characteristics of lightning activity for much of the Western Hemisphere (*see* figure 1).

Radio atmospherics, commonly known as "sferics," are the impulsive radio signals launched by lightning flashes. The new technology used for lightning location is known as "VLF Fourier Goniometry," a wideband frequency-domain method of arrival-bearing determination developed at Stanford as part of a Ph.D. dissertation (Burgess 1993). The application of VLF Fourier Goniometry to sferics measurements provides improved accuracy over earlier magnetic direction-finding techniques (Inan et al. 1996; Reising et al. 1996). Spherical geometric triangulation of arrival bearings of the same sferic measured at multiple receiving stations allows accurate (<200 km) location of individual lightning discharges. Flash rates can be measured continuously for individual storms over most of the Western Hemisphere from radio atmospheric measurements at Stanford, California, and at Palmer Station.

The luminous glows in the mesosphere above thunderclouds are known as "sprites" and are believed to be produced as a result of the heating of lower ionospheric electrons by intense quasielectrostatic fields, which exist at high altitudes above thunderstorms following lightning discharges (Pasko et al. 1995). Although sprites typically occur in associa-

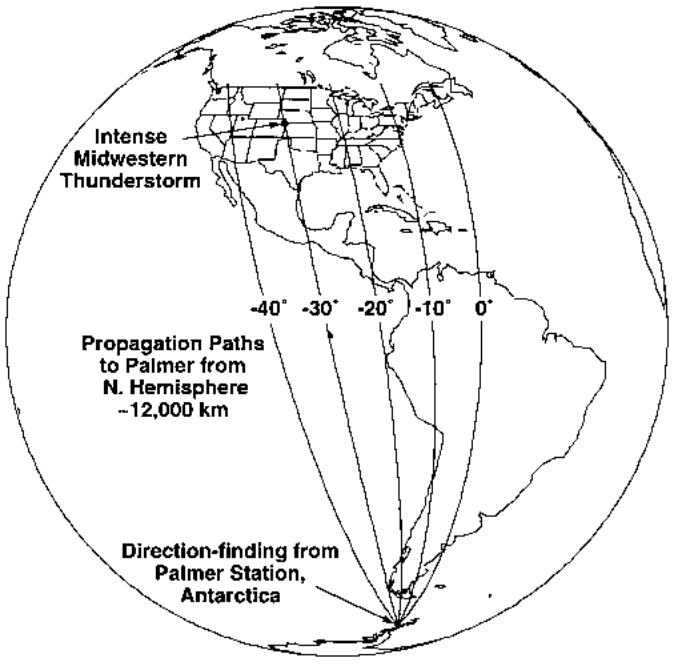

Figure 1. Geometry of Palmer Station observations of sferics originating in a midwestern U.S. thunderstorm approximately 12,000 km away. (Figure from Reising et al. 1996.)

tion with large positive-polarity cloud-to-ground (+CG) lightning flashes, many other large +CG flashes occur without any associated optical emissions. Reising et al. (1996) presented new measurements at Palmer Station, Antarctica, of the radio atmospheric waveforms of lightning discharges associated with sprites. Those results indicate that sprites are produced by those +CG flashes that excite radio atmospherics with an enhanced so-called "slow-tail" component (figure 2), indicating the presence of continuing current in the parent CG lightning. The continuing current is a longer lasting charge transfer to ground than the typical return stroke, which lasts less than 100 microseconds. Two sprite-producing mesoscale convective systems (MCS) over Nebraska were studied using optical data on sprite occurrence from Yucca Ridge, Colorado, and extremely-low-frequency (ELF) and VLF broadband data from Palmer Station, approximately 12,000 km from the source lightning (*see* figure 1). Using satellite-derived timing information accurate to better than 1 ms, hundreds of sferics were correlated one-to-one with first strokes of flashes detected by the National Lightning Detection Network (NLDN). For over 90 percent of the sferics, the arrival azimuths as measured using VLF Fourier Goniometry (*see* figure 3) were within ±1° (±200 km at 12,000 km range) of the measured NLDN flash locations (accurate to approximately 1 km). The efficiency of this method for lightning detection was demonstrated by measurement of VLF sferics in association with 80 percent of all NLDN-detected lightning flashes larger than 20 kiloamperes over a 2-hour period. VLF sferics were detected from intracloud (IC) lightning as well as from CGs, as shown by the number of sferics detected exceeding the stroke rate by a factor of more than 20.

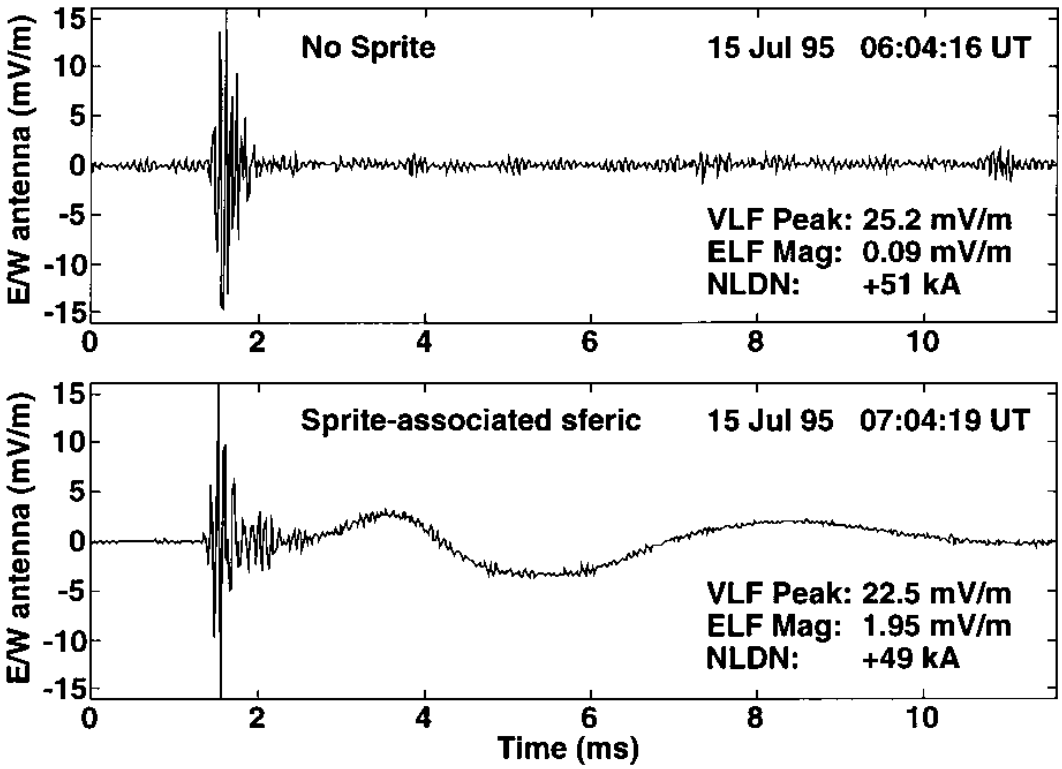

Figure 2. Waveforms of two sferics originating in the same storm over the midwestern United States and having similar VLF intensities but markedly different ELF intensities. The lower panel waveform exhibits a typical slow tail more than 20 times more intense than that in the upper panel. The waveform in the upper panel was associated with an optically recorded sprite, whereas the one in the upper panel was not. (Figure from Reising et al. 1996.) (mV/m denotes millivolts per meter. kA denotes kiloampere.)

Analysis by Reising et al. (1996) of more than 500 sferics that originated in CG return strokes demonstrated that the time-integrated ELF intensity of the sferics, measured at a distance of 12,000 km from the storm, serves as a proxy measure for the production of sprites. Optical/video measurements of sprites and other lightning-associated optical emissions are now typically conducted in the midwestern United States every June through August, and ongoing measurements at Palmer Station will be instrumental in investigating characteristics of the associated lightning discharges.

The strongest evidence of the coupling of lightning energy to the mesosphere/lower ionosphere comes from the first observations of gamma-ray flashes of terrestrial origin by the Compton Gamma Ray Observatory (GRO) (Fishman et al. 1994). Radio atmospheric data recorded at Palmer Station were used to confirm the presence of electrically active thunderstorms below the source regions of gamma-ray bursts detected

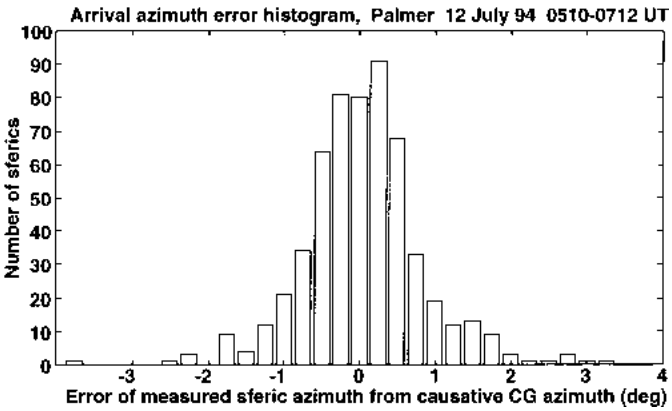

Figure 3. Histogram of error between arrival azimuths at Palmer Station using Fourier Goniometry and those derived from NLDN flash location data. The NLDN location error is insignificant on this spatial scale. (Figure from Reising et al. 1996.)

by GRO. In one case, a +CG flash having a large ELF component and resembling slow tails of sferics from sprite-producing lightning was identified in unambiguous association with a gamma-ray flash recorded by GRO (Inan et al. 1996).

We acknowledge the enthusiastic and capable support of our Palmer Station equipment by Kevin Bliss and John Booth, Antarctic Support Associates Science Technicians at Palmer Station for the past year. We thank John Lynch, National Science Foundation Program Manager, for his continued support. This work was supported by National Science Foundation grant OPP 93-18596-002.

References

Burgess, W.C. 1993. Lightning-induced coupling of the radiation belts to geomagnetically conjugate ionospheric regions. (Ph.D. Thesis, Stanford University, Department of Electrical Engineering, Stanford, California.)

Fishman, G.J., P.N. Bhat, R. Mallozzi, J.M. Horack, T. Koshut, C. Kouveliotou, G.N. Pendleton, C.A. Meegan, R.B. Wilson, W.S. Paciesas, S.J. Goodman, and H.J. Christian. 1994. Discovery of intense gamma-ray flashes of atmospheric origin. *Science*, 264, 1313.

Inan, U.S., C. Barrington-Leigh, S. Hansen, V.S. Glukhov, T.F. Bell, and R. Rairden. 1997. Rapid lateral expansion of optical luminosity in lightning-induced ionospheric flashes referred to as "elves." *Geophysical Research Letters*, 24, 583.

Inan, U.S., S.C. Reising, G.J. Fishman, and J.M. Horack. 1996. On the association of terrestrial gamma-ray bursts with lightning and implications for sprites. *Geophysical Research Letters*, 23, 1017.

Inan, U.S., J.V. Rodriguez, and V.P. Idone. 1993. VLF signatures of lightning-induced heating and ionization of the nighttime D-region. *Geophysical Research Letters*, 20, 2355.

Lyons, W.A. 1994. Characteristics of luminous structures in the stratosphere above thunderstorms as imaged by low-light video. *Geophysical Research Letters*, 21, 875.

Pasko, V.P., U.S. Inan, Y.N. Taranenko, and T.F. Bell. 1995. Heating, ionization and upward discharges in the mesosphere due to intense quasi-electrostatic thundercloud fields. *Geophysical Research Letters*, 22, 365.

Reising, S.C., U.S. Inan, T.F. Bell, and W.A. Lyons. 1996. Evidence for continuing currents in sprite-producing cloud-to-ground lightning. *Geophysical Research Letters*, 23, 3639.

Sentman, D.D., E.M. Wescott, D.L. Osborne, D.L. Hampton, and M.J. Heavner. 1995. Preliminary results from the Sprites 94 campaign: Red sprites. *Geophysical Research Letters*, 22, 1205.

Wescott, E.M., D. Sentman, D. Osborne, D. Hampton, and M. Heavner. 1995. Preliminary results from the Sprites 94 Campaign: Blue jets. *Geophysical Research Letters*, 22, 1209.

Balloonborne solar telescope circles Antarctica in 19 days

DAVID M. RUST, *Applied Physics Laboratory, The Johns Hopkins University, Laurel, Maryland 20723*

The Flare Genesis Experiment (FGE) is a new and versatile solar observatory. It can measure solar surface magnetic fields and motions with a unique balloonborne 80-centimeter (aperture) telescope (figure 1). By observing continuously for days from the antarctic stratosphere, above 99.7 percent of the atmosphere, the FGE overcomes the principal problems that have hindered solar magnetic field observations from the ground.

The principal objective of the FGE is to understand the origins of solar activity (Rust et al. 1993). How do fibrous and twisted magnetic fields emerge at the solar surface and how do they coalesce, unravel, and erupt as solar flares? Greatly improved magnetic field observations are needed to answer these questions. Higher spatial resolution, greater stability during observations, and longer runs without interruptions are expected to reveal key features of magnetic energy buildup and release on the Sun.

The FGE program will concentrate on magnetic field evolution, including the buildup of twist, or *helicity*, in the emerged fields (Rust 1994a). This effort may lead to reliable forecasts of solar activity and of the arrival of dangerous shocks and atomic particles at Earth.

Most of the time, existing solar telescopes have an effective angular resolution 10 times worse than the FGE's 0.2 arcsec (or 140 kilometers spatial resolution). Sometimes opportunities arise for sequences of a few minutes or half an hour of imaging with 0.3 arcsec or better, but it is probably impossible to follow solar magnetic field developments with such observations. The FGE is the only telescope that can consistently resolve field structures at the 140-kilometer level. Although not all the capabilities were realized on the first flight, in January 1996, the flight did make clear that the fundamental design approach of the FGE is sound.

The key high-technology optical elements are the lightweight, ultra-low-expansion primary mirror, the single-crystal silicon secondary mirror, the graphite-epoxy telescope tube, a tunable lithium-niobate optical filter (Rust 1994b), and an image motion compensator based on a novel silicon retina.

Major steps in the development of the FGE payload included acquisition of the 80-centimeter F/1.5 telescope from the Space Defense Initiative Office. It was built for flight on the space shuttle, and so it is very lightweight and thermally stable. It was given to the FGE program on indefinite loan and came with an invoiced value of $12 million. A major challenge was to design a cooling system for it. During the first flight, the secondary mirror never got above 37°C, which is amazing, considering that the intensity of the incident solar radiation on it was 60 times normal.

The gondola is a general-purpose solar balloon craft that can be duplicated by other experimenters for relatively minor

cost. It includes, among others, systems for solar fine-pointing, data recording, high-speed telemetry, power generation, and distribution.

The FGE flight yielded valuable data. The flight lasted from 7 to 26 January—one of the longest flights in Antarctica. We have processed and examined about half of the 14,000 images. In a 37-hour interval, the FGE obtained the longest uninterrupted, high-resolution record of solar convective flows. We did not record any solar activity (there was none), but future flights will take place nearer solar cycle maximum, when many targets will present themselves.

Steve Keil has begun analysis of the photospheric motions. His "cork" analysis benefits greatly from stable images and the long, uninterrupted run. Figure 2 shows the first results of his analysis, which attempts to follow the sideways motions of solar granules long enough to reveal the points of convergent motion. We should also be able to pinpoint regions of vortical flows and compare them with magnetograms obtained by other observatories. The results will be available on the World Wide Web at *http://sd-www.jhuapl.edu/FlareGenesis/*.

The FGE survived launch, descent, and landing without apparent damage, and the temperatures of key components remained in the safe operating range. The high-speed, line-of-sight uplink was maintained for 18 hours after launch, to a slant range of 490 kilometers. Downlink was maintained for 20 hours to a distance of 560 kilometers. The pointing servo controller maintained pointing for over 95 percent of the 19-day flight. The images from the first flight are not as sharp as they will be on future flights, but the recorded data are being corrected for this because we can deduce the focus error from the data.

Figure 1. The FGE ready for launch on 7 January 1996. The payload is about 5.5 meters high and weighs 1,900 kilograms. It is the largest payload flown in Antarctica.

At the end of the January 1996 flight, the FGE dropped gently into snow on the antarctic plateau 140 kilometers from Dumont d'Urville, the French base. The data tapes were recovered, but the rest of the payload could not be brought back, due to end-of-season departure of resources from Antarctica. In December 1996, the FGE was recovered by a French team from Dumont d'Urville and by Harry Eaton of the FGE staff. It now can be flown several more times before the next solar maximum. This is the inherent advantage in approaching space with a recoverable, balloonborne payload.

The FGE balloonborne telescope offers the least expensive means for probing solar activity for long intervals at high resolution. It is unique in its capacity to study solar activity in the approaching solar cycle.

Members of the Flare Genesis Experiment team in Antarctica were D. Rust, K. Strohbehn, G. Murphy, A. Kumar, R.

Cain, and H. Eaton of Johns Hopkins University's Applied Physics Laboratory; S. Keil and P. Wiborg of the Air Force Phillips Laboratory; C. Keller of the National Solar Observatory; and a team from the National Scientific Ballooning Facility. This work was supported by National Science Foundation grant OPP 91-19807 and Air Force Office of Scientific Research grants F49620-94-1-0079 and F49620-92-J-0284.

References

Rust, D.M. 1994a. Spawning and shedding helical magnetic fields in the solar atmosphere. *Geophysical Research Letters*, 21, 241–244.

Rust, D.M. 1994b. Etalon filters. *Optical Engineering*, 33, 3342–3348.

Rust, D.M., J.R. Hayes, D.A. Lohr, G.A. Murphy, and K. Strohbehn. 1993. The Flare Genesis Experiment: Studying the Sun from the stratosphere, *Johns Hopkins Applied Physics Laboratory Technical Digest*, 14(4), 358–369.

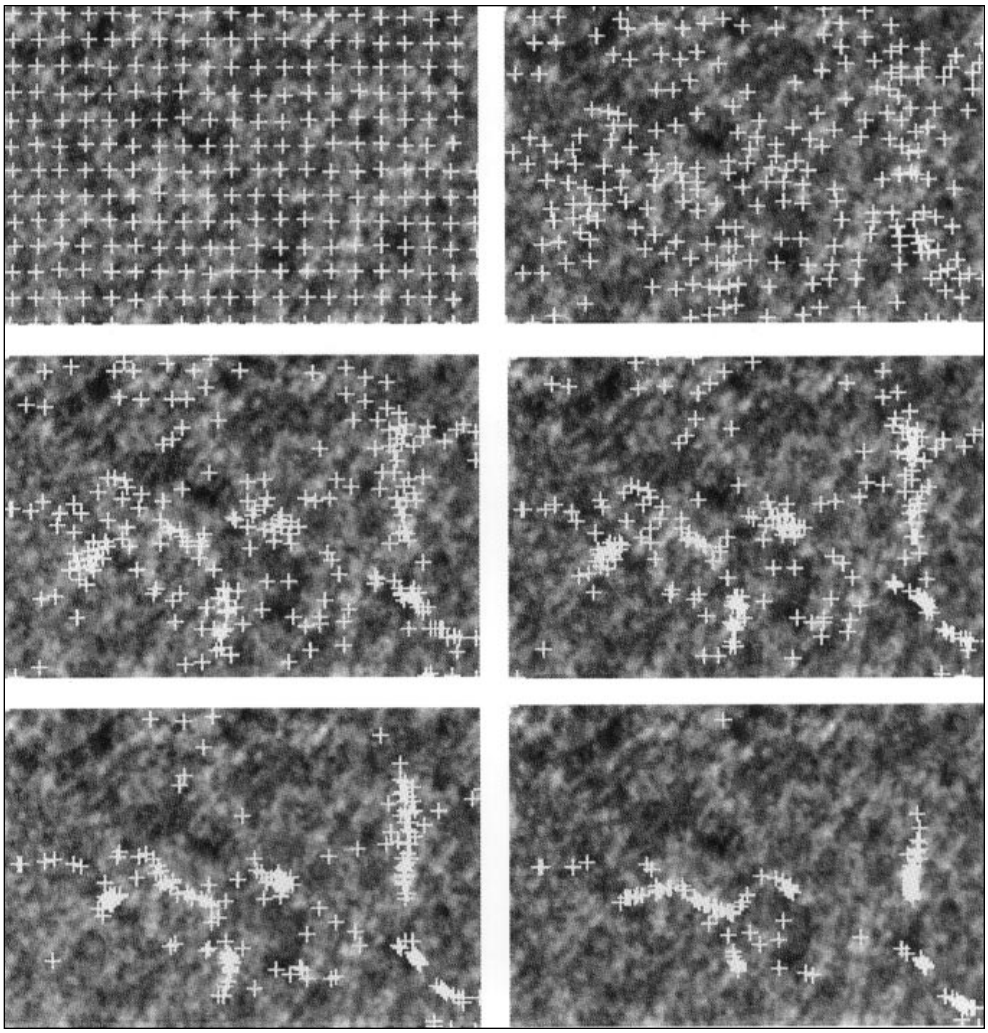

Figure 2. Upper left: first frame from the FGE movie, with computer-generated tracers ("corks") inserted in a regular pattern. The sequence of frames from upper left to lower right shows how magnetic flux ropes would likely cluster along probable convection cell boundaries in an 18-hour period. The solar area shown is 65,000 kilometers wide.

Deciphering the enigma of sunspot formation

S.M. JEFFERIES, *Bartol Research Institute, University of Delaware, Newark, Delaware 19716*

Sunspots are a well-known phenomena and have been routinely studied since the advent of the telescope at the beginning of the 17th century. These dark spots on the solar surface, which are caused by areas of cooler gas and stronger magnetic fields in the Sun's photosphere, come and go with a nominal 11-year periodicity: the so-called solar activity cycle. Because solar radiation is depleted in sunspots, any change in the number of sunspots gives rise to a change in the Sun's radiative energy output. In light of the growing evidence that variability in the Sun's radiative energy directly affects the biosphere (e.g., it causes changes in global surface temperatures and in the ozone layer), the importance of understanding sunspots is paramount. Despite this importance, our knowledge of just how sunspots form and are maintained is minimal. One popular theoretical model (Parker 1979) suggests that small vertical magnetic flux tubes, generated deep within the Sun, develop downflows around them when they emerge at the surface. These downflows bring together a large number of flux tubes in a cluster to form a sunspot, which then behaves as a single flux bundle as long as the downflows

bind the flux tubes together. Until now, it has not been possible to test the validity of this model.

The recent development of helioseismic tomography by our group (Duvall et al. 1996) now allows us to make subsurface observations and to produce three-dimensional maps of the solar interior. Helioseismic tomography is based on the measurement of the travel times of acoustic waves between different points on the solar surface (Duvall et al. 1993). As an acoustic wave propagates from its source near the solar surface into the interior, it refracts because of the increase in sound speed until it eventually turns around and returns to the surface where it is reflected back into the interior by the rapid change in density at the surface. This refraction and reflection of the wave continues until it has dissipated all of its energy. If the wave encounters a subsurface structure on its journey, such as a flow field, magnetic field, or temperature perturbation (which introduces an inhomogeneity in the wave speed along the path), its travel time will be altered. Because waves with different horizontal wavelengths penetrate to different depths of the solar interior, measurement of the travel time alterations can be used to generate a three-dimensional map of the perturbation. This map can then be used to locate and measure any subsurface structure.

Using calcium potassium-line intensity observations of the full solar disk, obtained at South Pole on 4–5 January 1991, we have generated travel-time maps for four different depths beneath the solar surface. An inversion of these maps (Kosovichev 1996), which are sensitive to flow velocities and perturbations in the sound speed, shows the presence of strong downflows beneath both sunspots and the bright features known as *plages*. The flows have a velocity of 1 to 2 kilometers per second and persist to a depth of about 2,000 kilometers. The data also suggest, however, that the vertical magnetic field can be a coherent flux bundle only to a depth of approximately 600 kilometers; below this depth it is possible that the downflows hold together a loose collection of flux tubes to maintain the sunspots that we see.

In summary, the new tomographic maps of the solar interior seem to verify Parker's model and provide the first step to understanding the nature of sunspots. Future high-resolution measurements will allow better depth resolution and are the obvious next step in this work.

The current South Pole helioseismology group consists of S.M. Jefferies, J.W. Harvey, T.L. Duvall, Jr., and M.F. Woodard. The success of our program over the past decade would not have been possible without the excellent help of the Amundsen–Scott South Pole Station support crew. This work was supported by National Science Foundation grant OPP 92-19515, the Solar Physics Branch of the Space Physics Division of the National Aeronautics Space Administration, and the National Solar Observatory.

References

Duvall, T.L., Jr., S.M. Jefferies, J.W. Harvey, and M.A. Pomerantz. 1993. Time-distance helioseismology. *Nature*, 362, 430.

Duvall, T.L., Jr., S. D'Silva, S.M. Jefferies, J.W. Harvey, and J. Schou. 1996. Downflows under sunspots detected by helioseismic tomography. *Nature*, 379, 235.

Kosovichev, A. 1996. Tomographic imaging of the Sun's interior. *Astrophysical Journal*, 461, L55.

Parker, E.N. 1979. Sunspots and the physics of magnetic flux tubes. I. The general nature of the sunspot. *Astrophysical Journal*, 230, 905.

Solar wind pressure and the generation of Pc 1 waves in the magnetosphere

ROGER L. ARNOLDY, *Space Science Center, University of New Hampshire, Durham, New Hampshire 03824*
MARK J. ENGEBRETSON *and* JENNY ALFORD, *Physics Department, Augsburg College, Minneapolis, Minnesota 55454*

Because our induction magnetometers have a sensitivity range for magnetohydrodynamic waves with periods of 1,000 seconds down to 0.2 seconds [millihertz (mHz) to 5 hertz (Hz)], they sense Pc 1 waves (0.2 to 5 Hz), which are generally not measured with conventional fluxgate magnetometers. Are Pc 1 waves important in the overall physics of the interaction of the magnetosphere with the solar wind? Conventional wisdom just 10 years ago would have said no, because it was believed that these waves were primarily generated by cyclotron resonance that has ring current protons at the plasmapause density gradient. The magnetic field measurements near the Earth's equatorial plane by the Ampte CCE spacecraft have drastically changed this view. The statistical study of Pc 1/2 waves by Anderson, Erlandson, and Zanetti (1992) showed that the majority of these waves measured near the equatorial plane by CCE were found at L shells near the spacecraft apogee, normally just inside the magnetopause. In addition, analyses of ground, high-latitude, induction magnetometer data have shown that bursts of Pc 1 waves are a common feature on the dayside at cusp latitudes. A correlation of Ampte CCE data with ground-induction magnetometer data from South Pole, Antarctica (Anderson et al. 1996) has shown remarkable temporal correspondence between these bursts recorded on the ground and in space near the dayside boundary of the magnetosphere. The conclusion from this work is that the Pc 1 bursts are generated at large L shells near the equatorial plane (pre-

sumably by ion cyclotron resonance) on closed field lines within a region about 2 hours wide including the subsolar point.

Further analysis of high-latitude induction magnetometer data (Arnoldy, Engebretson, and Cahill 1988) has shown that the Pc 1 bursts are related to magnetic impulse events (MIE) recorded on the ground. The MIE are one- to two-cycle magnetic signals that have periods in the Pc 5 range (a few to several minutes). In an analysis of about 2 years of high-latitude data, we have shown that about 70 percent of all MIE have an associated Pc 1 burst (Arnoldy et al. 1996). This same study compared a ground Pc 1 burst and MIE with Viking spacecraft data taken over the ground station at an altitude of 13,000 kilometers. In space, the Pc 1 waves were spatially separated from the MIE. The Pc 1 burst occurred on closed field lines and the MIE on the electron-trapping boundary well equatorward of the dayside cusp. It appears as if the trigger for the generation of the MIE and the Pc 1 burst might be the same, but the generation region of the two signals is not the same. It is still uncertain if the MIE are the ground signature of bursty dayside magnetic reconnection, solar wind pressure pulses, or the intrusion of magnetosheath plasma into the magnetosphere.

Because it is now apparent that Pc 1 waves may be an important new wavelength to study the solar wind-magnetosphere coupling mechanism, we have commenced a study of solar wind parameters measured by the Wind spacecraft and the occurrence of Pc 1 waves in the magnetosphere as measured on the ground at high latitudes. In the figure, the ground-induction magnetometer data from our Canadian Iqaluit station, located at 70° north invariant latitude, readily affirms the strong control the solar wind has on the generation of these waves in the magnetosphere. This figure consists of frequency vs. time spectrograms of the y-axis pulsation data for an entire day upon which is superimposed, as a line plot, the Wind spacecraft measurement of solar wind dynamic pressure. The pressure plot is displaced in time to account for the travel time of the solar wind from the spacecraft to Earth, a distance of about 30 Earth radii (R_e). The top panel is the night quadrant for the station, and sequentially, the panels represent the dawn, noon, and dusk sectors because local magnetic midnight for the station occurs at 0330 univeral time (UT).

The spectrograms nicely show "a day in the life" of a ground, high-latitude pulsation sensor. In the night quadrant, the bursts of Pi waves are directly related to overhead auroral displays. Because these events have no immediate one-to-one correlation with the solar wind dynamic pressure, we have not plotted pressure in this panel. The next three time sectors, however, typically have band-limited pulsation signals which, as the figure clearly shows, are correlated with the solar wind pressure. At about 1 hour before local dawn (0800 UT), the burst of Pc 1 waves of 0.6-Hz frequency is clearly correlated with a burst of dynamic pressure in the solar wind. Later in this sector, the gradual increase in solar wind pressure seems to be related to the occurrence of Pc 1/2 waves between 1000 and 1200 UT. Following local magnetic noon, at 1530 UT, a very bursty and patchy Pc 1 power occurs, and its maximum frequency has a clear correlation with the magnitude of the solar wind pressure. In the dusk

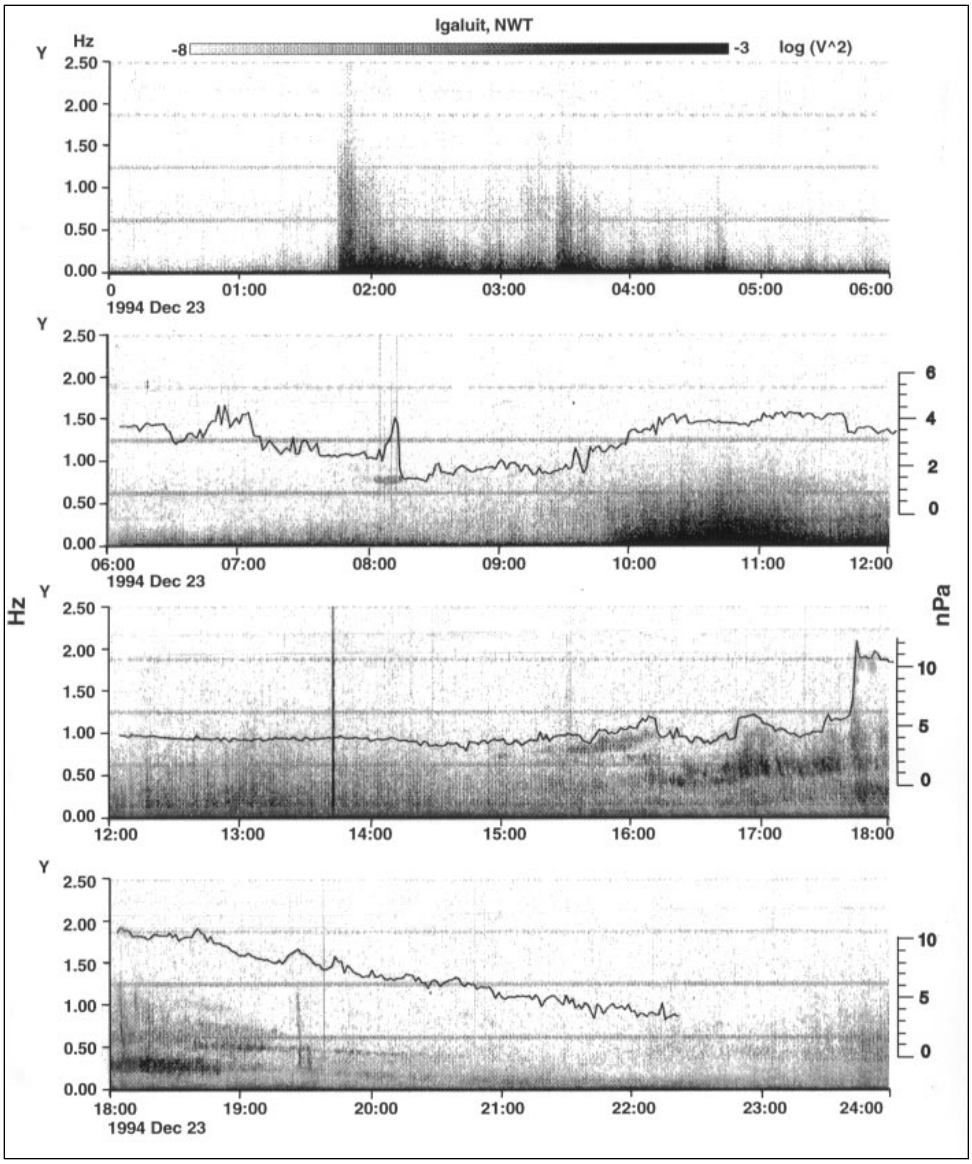

Frequency vs. time spectrograms for 23 December 1994 with superimposed solar wind dynamic pressure. The left scale has units of frequency while the right scale has units of nanopascals for the pressure plot.

sector, several of the Pc 1 bursts (1805, 1810, 1925 UT) of minutes duration might be related to fluctuations in the pressure. Finally, also in this sector, two narrow-bandwidth emissions, lasting for hours, decrease in frequency as the solar wind dynamic pressure decreases. In summary, this plot contains a wealth of information about Pc 1 waves and their relationship to the solar wind.

Correlations of Pc 1 waves and solar wind parameters are not always as striking as the example given in the figure. The defining condition for good correlation seems to be that the Wind spacecraft has to be within a few tens of R_e ahead of the bow shock and within 10 R_e of Sun-Earth line. Historically, the correlation of ground pulsation data with the solar wind parameters as measured by the IMP 8 spacecraft, which now seems to be related to the rather large Y-values of the spacecraft when it was ahead of the bow shock, has been only partially successful. It is intriguing that one might be able to infer solar wind pressure fluctuations by looking at ground Pc 1 data collected at high latitudes. As an example, the famous "spaceweather" event when the Canadian Anik spacecraft at synchronous orbit was perturbed by geophysical events has no accompanying solar wind data to determine the status of the interplanetary medium. In analyzing our ground-induction magnetometer data, however, it is found that on 21 January 1994, prior to the spacecraft malfunctions, a sudden appearance of 1.5 Hz Pc 1 waves occurs, and that suggests a dramatic increase in solar wind dynamic pressure similar to what happened in the figure at 1745 UT.

This research was supported by National Science Foundation grant OPP 92-17024.

References

Anderson, B.J., R.E. Erlandson, M.J. Engebretson, J. Alford, and R.L. Arnoldy. 1996. Source region of 0.2 to 1.0 Hz geomagnetic pulsations bursts. *Geophysical Research Letters*. 23(7), 769–772.

Anderson, B.J., R.E. Erlandson, and L.J. Zanetti. 1992. A statistical study of Pc 1/2 magnetic pulsations in the equatorial magnetosphere: 1. equatorial occurrence distributions. *Journal of Geophysical Research*, 97, 3075–3088.

Arnoldy, R.L., M.J. Engebretson, J.L. Alford, R.E. Erlandson, and B.J. Anderson. 1996. Magnetic impulse events and associated Pc 1 bursts at dayside high latitudes. *Journal of Geophysical Research*, 101, 7793–7799.

Arnoldy, R.L., M.J. Engebretson, and L.J. Cahill, Jr. 1988. Bursts of Pc 1/2 near the ionospheric footprint of the cusp and their relationship to flux transfer events. *Journal of Geophysical Research*, 93, 1007–1016.

Patterns in high-latitude observations of Pc 1–2 emissions

MARK J. ENGEBRETSON *and* LARS P. DYRUD, *Department of Physics, Augsburg College, Minneapolis, Minnesota 55454*
PATRICK T. NEWELL, *The Johns Hopkins University Applied Physics Laboratory, Laurel, Maryland 20723*
W. JEFFREY HUGHES, *Center for Space Physics, Boston University, Boston, Massachusetts 02215*
ROGER L. ARNOLDY, *Space Science Center, University of New Hampshire, Durham, New Hampshire 03824*
HIROSHI FUKUNISHI, *Upper Atmosphere and Space Research Laboratory, Tohoku University, Sendai 980, Japan*

The extension of the Earth's magnetic field into space is bounded by its interaction with the solar wind, which itself carries a magnetic field that originates in the Sun. The interaction of these magnetic fields and the plasmas that are bound up with them causes significant distortions of the Earth's exterior magnetic field (the magnetosphere), frequently generates auroral displays, and occasionally causes severe electromagnetic disruptions to human power and communications systems. Magnetic field lines at the boundary map to the polar cusps, small regions near 75° magnetic latitude at local noon in the Northern and Southern Hemispheres. These cusp regions are the focus of much ground-based research because researchers believe the regions will provide diagnostics of plasma interactions at this remote and invisible boundary.

Although magnetic field oscillations (pulsations) in the Pc 1–2 frequency range [100–600 millihertz (mHz)] have been studied at lower latitudes for many years, observations at cusp latitudes have been limited. Recent experimental initiatives supported by the National Science Foundation have funded the installation of arrays of sensitive ground-based magnetometers that rotate under these cusp regions daily. The polar experiment network for geophysical upper atmosphere investigations (PENGUIN) array of automatic geophysical observatories (AGOs) in Antarctica (Rosenberg and Doolittle 1994) and the magnetometer arrays for cusp and cleft studies (MACCS) in Arctic Canada (Engebretson et al. 1995) provide roughly conjugate observations of the cusp and nearby regions.

Menk et al. (1992) suggested that the cusp could be identified in ground records from the presence of one class of Pc 1–2 waves, with relatively broadband and unstructured appearance. To test this suggestion, we surveyed a full year's data from the MACCS and PENGUIN arrays. We found latitudinal differences similar to those found in the Menk et al. (1992) study, in that magnetometers at very high magnetic latitudes (near 80° magnetic latitude) most commonly observe broadband diffuse Pc 1–2 waves, and those near 75° most commonly observe narrowband Pc 1–2 waves. Other details of our data,

however, led us to propose a different source for the broadband waves.

Figure 1 is a map of the antarctic scientific stations with the PENGUIN AGO stations enlarged and represented by squares. The MACCS stations, denoted by solid circles, have been mapped using corrected geomagnetic coordinates and superimposed on their conjugate antarctic sites. Magnetic lines of latitude and longitude are represented by bold lines.

A statistical study of 1994 data from four MACCS stations and AGO P1 and P4 showed a semiannual variation in event occurrence and showed that 95 percent of Pc 1–2 events occurred within approximately 5 hours of local noon and within a frequency range of 120–250 mHz. A histogram for the entire year (figure 2) shows that Pc 1–2 waves observed at AGO P1 and Clyde River (CY), with magnetic latitudes near 80°, had significantly wider bandwidth than waves observed at stations such as Cape Dorset (CD), near 75°. The stations at higher latitudes also showed a relative lack of very narrowband waves (25–100 mHz in bandwidth).

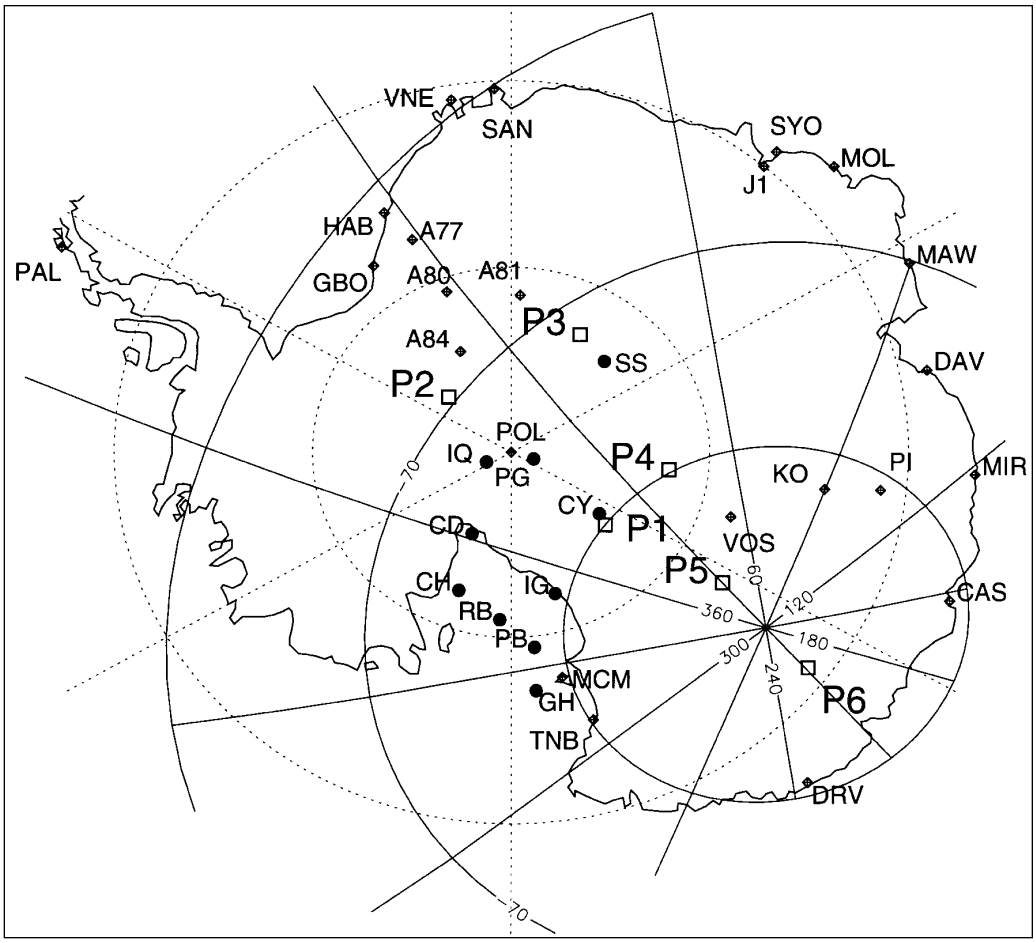

Figure 1. Map of scientific stations in Antarctica. The PENGUIN AGO stations are represented by squares. The MACCS stations, denoted by crosses, have been mapped using corrected geomagnetic coordinates and superimposed on their conjugate antarctic sites. Magnetic lines of latitude and longitude are represented by bold lines.

Figure 3 is a typical example of a day showing both wave types. Waves with wide bandwidth appear a few hours before local noon [1530 universal time (UT)] at AGO P1 in Antarctica and Clyde River in Canada, both near 80° magnetic latitude, and narrowband waves occur slightly later at Cape Dorset, near 75° magnetic latitude. On this day, all five available stations at magnetic latitudes above 78° show such semistructured broadband Pc 1–2 waves, while all stations at magnetic latitudes between 73° and 76° show narrowband waves during the same interval. The lower panel of figure 3 shows data from the Defense Meteorological Satellite Program (DMSP) satellites, which identify different regions of the magnetosphere by ion and electron signatures. These data show that from 14 to 16 UT stations at 80° are under the mantle region and polar cap field lines, while stations near 75° are near the boundary between the mantle and regions equatorward of

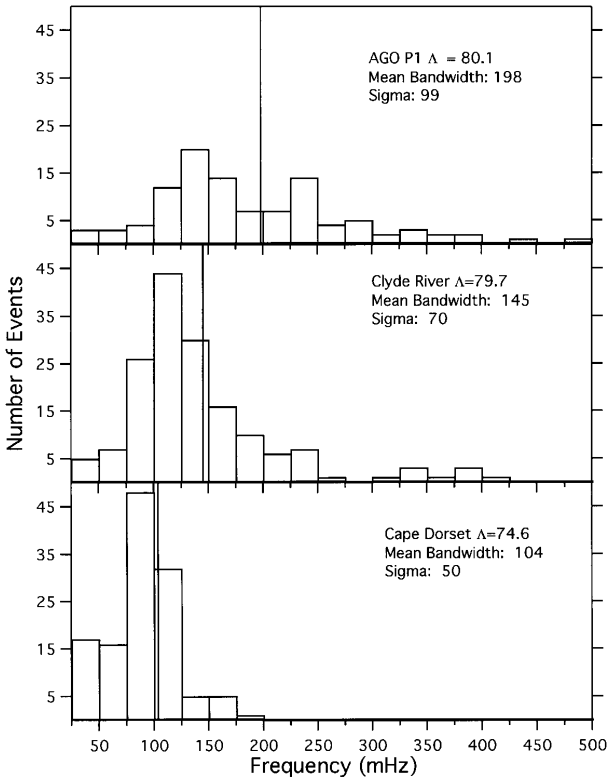

Figure 2. Histograms of Pc 1–2 pulsation bandwidth at AGO P1, Antarctica, and Clyde River and Cape Dorset, Canada, showing wider bandwidth waves at higher magnetic latitudes. The average value is shown by the vertical line.

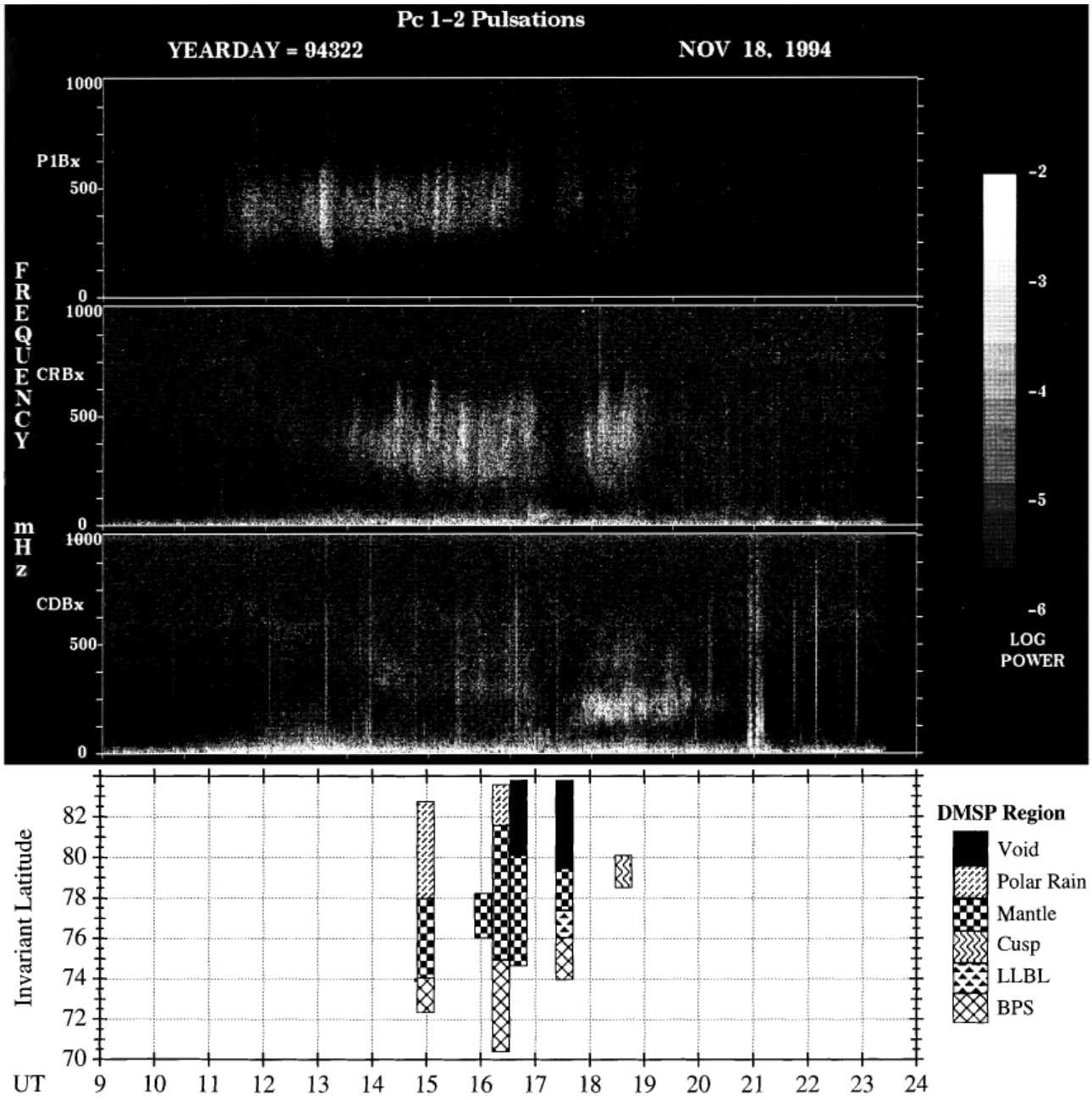

Figure 3. An example of multistation observations of a Pc 1–2 wave event. The 3-panel spectrograms are produced by a 256-point Fast Fourier Transform; the y-axis scale is in millihertz (mHz), the x-axis represents universal time (UT), and wave power is displayed by brightness using a logarithmic scale. Each panel displays the BX component from the magnetometer at the respective stations. The spectrogram panels are ordered from the highest latitude station at the top to the lowest latitude station at the bottom. The bottom panel summarizes DMSP satellite identifications of magnetospheric regions during the same time period. Regions equatorward of the cusp are denoted as BPS (boundary plasma sheet) and LLBL (low-latitude boundary layer), whereas regions poleward of the cusp are denoted as Mantle or Polar Rain.

the cusp. The cusp itself was not identified in any satellite passes until 1740 UT.

This event is typical of our findings: the plasma mantle and/or polar cap regions are over MACCS and AGO stations that observe wideband Pc 1–2 waves, and the low-latitude boundary layer and/or equatorward edge of the cusp are over stations that observe narrowband Pc 1–2. These observations lead us to believe that the plasma mantle, and not the cusp, is the source region for broadband Pc 1–2 waves observed at very high latitudes.

Recent theoretical work by Denton, Hudson, and Roth (1992) on ion cyclotron instabilities, which are believed responsible for generating Pc 1–2 waves, also supports a mantle source of these waves. Although large fluxes of ions flow downward in the cusp, this theory suggests that the waves they create will move in the opposite direction, hence upward and away from Earth. The cusp is thus probably not a good source for downgoing Pc 1–2 waves. Many downgoing cusp ions, however, are convected toward higher latitudes and are subsequently reflected back up into space in the mantle

region, poleward of the cusp. It is thus reasonable that downward propagating ion cyclotron waves can be generated by upgoing reflected ions in this region. Further studies using the full arrays of cusp-latitude stations will help to verify these conclusions and possibly lead to better ground-based diagnostics of the cusp region and the boundary of the Earth's magnetic field.

This research was supported by National Science Foundation grants OPP 89-18689, OPP 92-17024, and ATM 94-00664.

References

Denton, R.E., M.K. Hudson, and I. Roth. 1992. Loss-cone driven ion cyclotron waves in the magnetosphere. *Journal of Geophysical Research*, 97, 12093–12103.

Engebretson, M.J., W.J. Hughes, J.L. Alford, E. Zesta, L.J. Cahill, Jr., R.L Arnoldy, and G.D. Reeves. 1995. MACCS observations of the spatial extent of broadband ULF magnetic pulsations at cusp/cleft latitudes. *Journal of Geophysical Research*, 100, 19371–19386.

Menk, F.W., B.J. Fraser, H.J. Hansen, P.T. Newell, C.-I. Meng, and R.J. Morris. 1992. Identification of the magnetospheric cusp and cleft using Pc 1–2 ULF pulsations. *Journal of Atmospheric and Terrestrial Physics*, 54, 1021–1042.

Rosenberg, T.J., and J.H. Doolittle. 1994. Studying the polar ionosphere and magnetosphere with automatic geophysical observatories: The U.S. program in Antarctica. *Antarctic Journal of the U.S.*, 29(5), 347–349.

Low-frequency auroral hiss observations at high geomagnetic latitudes

JAMES LABELLE, JILL-ANNE PERRING, *and* MICHAEL TRIMPI, *Department of Physics and Astronomy, Dartmouth College, Hanover, New Hampshire 03755-3528*

A.T. WEATHERWAX, *Institute for Physical Science and Technology, University of Maryland, College Park, Maryland 20742-2431*

The best known auroral radio emission observed at ground level is auroral hiss, which is often observed together with auroral roar and mid-frequency (MF) bursts during auroral substorm onsets. Auroral hiss is of two types: continuous and impulsive (see review by Sazhin, Bullough, and Hayakawa 1993). The continuous type lasts an order of an hour or more and is usually restricted to very low frequencies (VLF). The impulsive type occurs during substorm onsets and consists of bursts of impulsive emissions lasting from a few seconds to tens of minutes. Impulsive auroral hiss often extends into the low-frequency (LF) range; for example, Jorgensen (1968) reports observations of LF hiss exceeding 500 kilohertz (kHz) at Byrd Station, Antarctica. Modern wave receivers in Antarctica and elsewhere detect auroral hiss at frequencies exceeding 1 megahertz (MHz). Although much auroral hiss may be explained by coherent amplification of whistler mode waves by auroral electrons (Maggs 1976), there exist rocket and satellite observations that cannot be satisfactorily explained by this model (Morioka and Oya 1985; Ergun et al. 1991).

LF auroral hiss observations in Antarctica are of particular interest, because only in the remote Antarctic can ground-based instruments detect natural LF signals; at Northern Hemisphere sites, the LF band is obscured by broadcast signals in the frequency ranges 550–1,600 kHz and 200–400 kHz. Dartmouth College operates low-frequency/mid-frequency/high-frequency (LF/MF/HF) receivers at three of the U.S. automatic geophysical observatories (AGOs): P1, P2, and P4. South Pole, located under the daytime cusp, is potentially an interesting site for radio observations, but station-generated interference obscures all but the strongest auroral roar and hiss events there. Starting in 1996, LF/MF/HF observations are also being conducted at the British AGOs A-80 and A-81.

By inspection of daily survey plots of AGO-P1 LF/MF/HF wave data, supplemented with specially produced plots of expanded resolution when needed, we generated a database of 121 impulsive LF auroral hiss events exceeding 30 nanovolts per meter per root hertz (nV/m$\sqrt{Hz}$) (intense events) and 370 events in the range 10–30 nV/m$\sqrt{Hz}$ (medium events). A far greater number of weak events (<10 nV/m$\sqrt{Hz}$) occur, not included in the database. Bursts of LF hiss had to occur 10 minutes apart to count as separate events. While identifying LF hiss events, we accumulated a parallel database containing all time intervals when LF auroral hiss exceeding 10 nV/m$\sqrt{Hz}$ was not observable because of various effects such as broadcast band interference, snow-static, or lack of data. The hours when auroral hiss was not observable were used to normalize the occurrence statistics of the LF hiss, which are presented below in units of hiss events per hour of valid data.

Figure 1 (*top*) shows that the occurrence rate of LF auroral hiss peaks in the premidnight hours (magnetic local time), consistent with previous observations of LF hiss (figure 3 of Morgan 1977a) and VLF hiss (e.g., Jorgensen 1966; Makita 1979). Figure 1 (*bottom*) shows the seasonal variation of the occurrence rate. The peak in austral winter (June/July) is consistent with previous observations, but we find a weak sec-

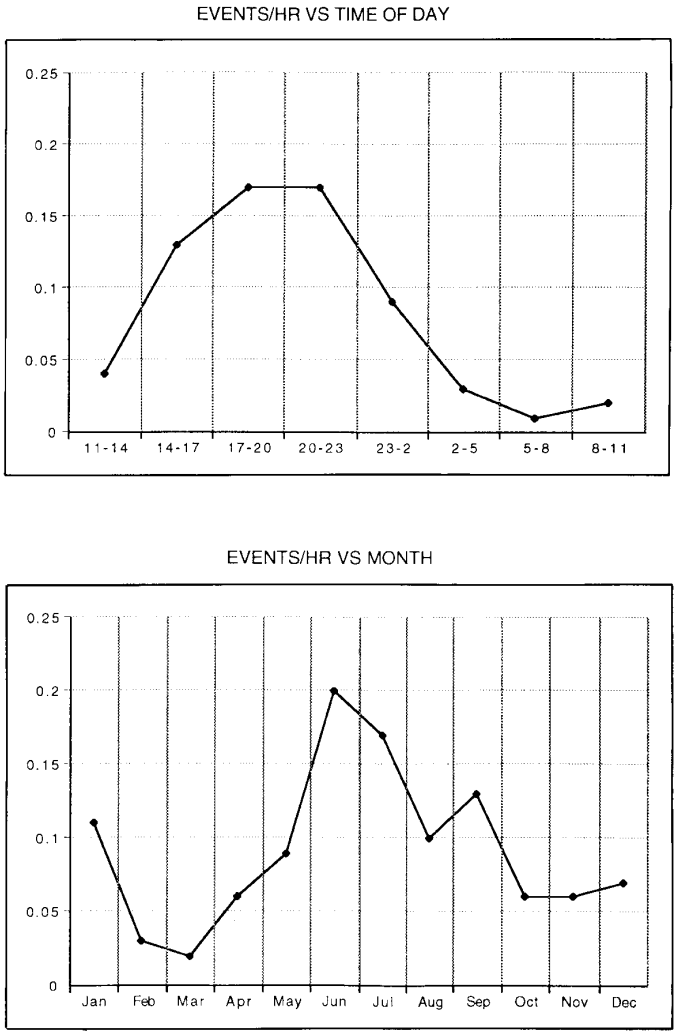

Figure 1. (*Top*) The occurrence rate of LF auroral hiss at AGO-P1 as a function of local time, based on data from January and December 1994. (*Bottom*) The occurrence rate of LF auroral hiss versus month of the year during 1994. The diurnal variation peaks in the premidnight hours, in agreement with previous studies. The seasonal variation peaks in austral winter as expected, but the weak peak in austral summer requires further analysis.

ondary peak in the occurrence rate during the conjugate hemisphere winter, not observed by Makita (1979) at VLF frequencies at Syowa Station (Makita's figure 12*B*). Another year of AGO data will allow a better assessment of the statistical significance of the austral summer secondary peak in the auroral hiss occurrence rate observed at high latitude.

Figure 2 shows a case study of auroral hiss bursts observed at AGO-P4 and AGO-P1 during 00-06 universal time (UT) on 30 May 1994 (corresponding approximately to 20-02 magnetic local time at P1 and 22-04 magnetic local time at P4). Mode changes cause gaps in the AGO-P4 spectrogram. Also displayed in figure 2 are two channels of VLF data (30–40 kHz and 2–4 kHz, respectively) and the north-south (H) components of the search coil magnetometer and flux-gate magnetometer, all measured at AGO-P1. The magnetometers detect activity starting at 0100–0130 UT and 0505–0515 UT, and impulsive auroral hiss is observed at these same times.

These events illustrate two spectral types of LF impulsive hiss events observed at ground-level. The event at 0100–0130 is primarily of the "normal" type, in which the peak intensity is at VLF frequencies, below the range of the LF/MF/HF instrument. During 0045–0105 UT, the event is observed exclusively on VLF; only after 0105 are both LF and VLF impulsive emissions detected. For a short time around 0120–0125 UT, the second spectral type occurs, which we call "LF cutoff," in which the dominant waves are at frequencies above 100 kHz, and VLF waves are weak or absent. In contrast, the 0515 event consists mostly of the LF cutoff type, with the highest auroral hiss intensity at 200–250 kHz except for one spike in the middle of the event which is particularly evident in the AGO-P4 spectrogram. The VLF channels register no activity except for the spike in the middle of the event. So although both events in figure 2 represent a mix of spectral types, the early 0100–0130 event consists primarily of the normal spectral type, whereas the later 0515 event consists primarily of the LF-cutoff type.

Inspection of 1994 AGO-P1 LF auroral hiss database reveals that the LF-cutoff type constitutes 13 percent of the medium-to-intense LF auroral hiss events. An additional 15 percent of the auroral hiss events are mixed types, like the examples in figure 2. The remaining 72 percent of the events are the normal type whose spectrum peaks at VLF frequencies. These statistics show that the type of hiss with a spectral peak at LF frequencies is not rare. In fact, it is well-known that auroral hiss observed at ground level exhibits a low-frequency cutoff, and Morgan (1977b) reports that in many examples detected at Frobisher Bay (approximately 75° magnetic latitude), the low-frequency cutoff is too high to be seen on audio frequency records. Case studies of AGO data, including, for example, the imaging riometer data, which provides information about ionospheric structure, may help determine whether the spectral signature of these events results from the generation mechanism or from propagation effects.

Antarctic AGO measurements at low frequencies reveal significant new features of impulsive auroral hiss emissions. The rate of occurrence of these emissions at 80° invariant is itself noteworthy. The diurnal and seasonal

Figure 2. A case study of LF auroral hiss bursts occurring on 30 May 1994 (00–06 UT) at AGO-P1 and AGO-P4. Gaps in the AGO-P4 spectrogram are caused by mode changes. The bottom four panels show integrated power over two VLF bands, ultra-low-frequency (ULF) magnetic fluctuations and the H-component of the geomagnetic field. Some of the auroral hiss bursts are detected by both the VLF and LF receivers; these represent the normal type of auroral hiss, which maximizes at VLF frequencies. (In some instances, such hiss events are observed only at VLF.) A second type of auroral hiss burst appears to maximize near 200 kHz in the LF wave spectrogram and is registered weakly or not at all by the VLF receiver.

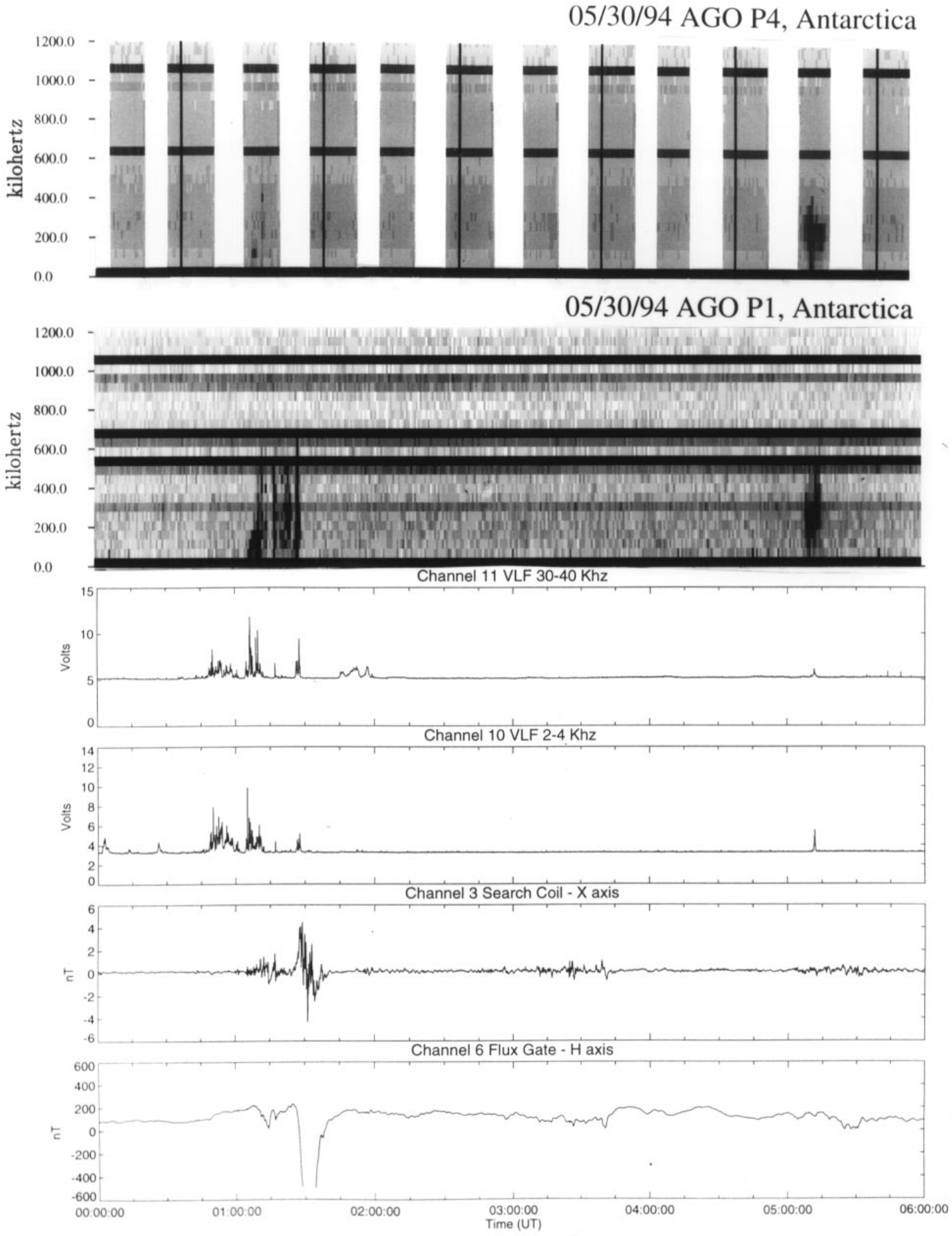

P1 May 30, 1994 Day 150

dependences of this occurrence rate roughly agree with that determined for VLF hiss at auroral latitudes. A secondary peak in the summer months has not been reported before but needs confirmation. The most significant contribution of the antarctic AGO observations is their resolution of the spectrum of the auroral hiss at LF, which is not possible at Northern Hemisphere sites due to manmade interference sources. A class of impulsive hiss events occurs for which the power spectral density peaks near 200–250 kHz; in some cases, the VLF component of these events is entirely undetectable. These "anomalous" events are not rare but constitute 15–28 percent of the medium to intense events observed.

The authors thank the AGO/polar experimental network for geophysical upper atmosphere investigations (PENGUIN) investigator team, especially H. Fukunishi, U. Inan, and L. Lanzerotti, for providing their data in support of this paper. This research was supported by National Science Foundation grants OPP 93-17621 to Dartmouth College and OPP 89-18689 to the University of Maryland. Jill-Anne Perring received support from the Women-in-Science Program at Dartmouth College.

References

Ergun, R.E., E. Klementis, C.W. Carlson, J. McFadden, and J.H. Clemons. 1991. Wavelength measurement of auroral hiss. *Journal of Geophysical Research*, 96, 21299.

Jorgensen, T.S. 1966. Morphology of VLF hiss zones and their correlation with particle precipitation events. *Journal Geophysical Research*, 71, 1367.

Jorgensen, T.S. 1968. Integration of auroral hiss measured at OGO 2 and at Byrd Station in terms of incoherent Cerenkov radiation. *Journal of Geophysical Research*, 73, 1055.

Maggs, J.E. 1976. Coherent generation of VLF hiss. *Journal of Geophysical Research*, 81, 1707.

Makita, K. 1979. VLF/LF hiss emissions associated with aurora, *Memoirs of the National Institute for Polar Research*, series A, number 16.

Morgan, M.G. 1977a. Wide-band observations of LF hiss at Frobisher Bay. *Journal of Geophysical Research*, 82, 2377.

Morgan, M.G. 1977b. Auroral hiss on the ground at L=4. *Journal of Geophysical Research*, 82, 2387.

Morioka A., and H. Oya. 1985. Emissions of plasma waves from VLF to LF ranges in magnetic polar regions—New evidence from the EXOS-C satellite. *Journal of Geomagnetism and Geoelectricity*, 37(3), 263.

Sazhin, S.S., K. Bullough, and M. Hayakawa. 1993. Auroral hiss: A review. *Planetary and Space Science*, 41(2), 153.

Characteristics of localized ionospheric disturbances deduced from very-low-frequency radio measurements at Palmer Station

S. LEV-TOV *and* U.S. INAN, *Space, Telecommunications, and Radioscience Laboratory, Stanford University, Stanford, California 94305*

Palmer Station for many years has provided Stanford University with a unique site for extremely-low-frequency (ELF) and very-low-frequency (VLF) radio wave observations. The outstanding features of Palmer Station are that it is an electromagnetically quiet site, which allows the making of very sensitive measurements, and that the location is geomagnetically conjugate to many Northern Hemisphere thunderstorm centers (which are over the east coast of the continental United States). These sensitive measurements are useful for recording electromagnetic waves from the magnetosphere, particularly whistler waves (Burgess and Inan 1993 and references therein) caused by lightning.

Measurements are conducted of both narrow- and broadband signals. Broadband signals measured are radio atmospherics (or spherics, which propagate through the Earth-ionosphere waveguide) and whistler waves, both of which are generated by lightning pulses. Narrowband signals measured are manmade VLF radio communication signals, which propagate through the Earth-ionosphere waveguide over large distances; spherics also appear on the narrowband records.

The narrowband signals provide a means for observation of the ionosphere at the altitude range of 60–100 kilometers (km), a difficult area in which to take measurements. We are particularly interested in the observation of localized disturbances caused by lightning-induced electron precipitation (LEP). Whistler waves generated by Northern Hemisphere lightning propagate through the magnetosphere and interact with electrons, which constitute part of the Earth's geomagnetically trapped radiation (the radiation belts). The electrons are then scattered in pitch angle, lowering their mirroring height, causing them to enter the atmosphere. These energetic electrons cause secondary ionization which modifies the ionosphere in a local region. These are ionospheric disturbances, and they are observed as perturbations of both amplitude and phase of the VLF signals. An example of the narrowband displays of LEP signatures and broadband displays of associated whistlers is shown in figure 1.

The broadband recordings of whistler waves provide characteristics of the waves themselves (such as the L-shell of propagation) that are responsible for the LEP and, when two

crossed magnetic loop antennas (one oriented north-south and the other east-west) are used, also provide a means to identify the direction of arrival of these waves. Establishing the direction of arrival locates the exit point of the duct (region of enhanced electron concentration along a magnetic field line) through which the whistler wave propagated. Knowing the L-shell of propagation and direction of arrival, along with knowing the location of the perturbed VLF path, helps to identify the location of the LEP disturbances.

LEP disturbances are a link between the magnetosphere and the ionosphere. Gaining information about the disturbances such as their rate of occurrence, their size, and their intensity provides a means of understanding the role that LEP plays as a loss of electrons to the radiation belts, as well as an indication of how much LEP occurs on a global scale.

Recent work (Lev-Tov et al. 1996) involving measurements taken at Palmer Station and the British Faraday Station have yielded further information about these disturbances (figure 2). Having narrowband data from the same disturbances on the same VLF signal (from the 23.4-kilohertz transmitter, which has the call letters NPM and is located in Hawaii) gave us a new perspective. The differences between amplitude and phase changes at the two stations shed new light on the LEP disturbances. Likely size, location, and the electron density altitude profile of the disturbance were deduced. For the first time, the effect of the day-night terminator (LEP events are visible only at night because of the lowered ionospheric VLF reflection height during the daytime) was considered in locating the disturbances and deducing some of their characteristics. Also, the disturbances seemed to move over time, providing the first observation by LEP of duct motion. This observation was not possible with just one VLF receiving station.

With collaboration from Brazilian and British colleagues, we are looking forward to using this multireceiver technique in the Southern Hemisphere in the future. The British Rothera Station and the Brazilian Commandante Ferraz Station will both take narrowband VLF measurements (figure 3). With three stations, even more details of LEP perturbations on VLF signals should be apparent. Also, we will be able to monitor a larger area than before (these three stations are farther apart than are Palmer and Faraday at approximately 50 kilometers).

This configuration of VLF receivers will complement Stanford University receivers in the Northern Hemisphere. LEP is a phenomenon that occurs in conjugate areas: because of differences in the strength of the Earth's magnetic field at conjugate LEP regions, the mirroring height of electrons in these regions may differ resulting in LEP in both regions. We can thus have a complete assessment of the amount of precipitated energetic electrons that originate from a single lightning strike.

Further study of LEP is provided by modeling the recovery signatures of LEP events. We will also be doing simultaneous ground-satellite observations of the LEP events.

We are grateful to the Antarctic Support Associates who have maintained our equipment at Palmer Station. This work is supported under National Science Foundation grant OPP 93-18596 to Stanford University.

References

Burgess, W.C., and U.S. Inan. 1993. The role of ducted whistlers in the precipitation loss and equilibrium flux of radiation belt electrons. *Journal of Geophysical Research*, 98(A9), 15643.

Lev-Tov, S.J., U.S. Inan, A.J. Smith, and M.A. Clilverd. 1996. Characteristics of localized ionospheric disturbances inferred from VLF measurements at two closely spaced receivers. *Journal of Geophysical Research*, 101(A7), 15737.

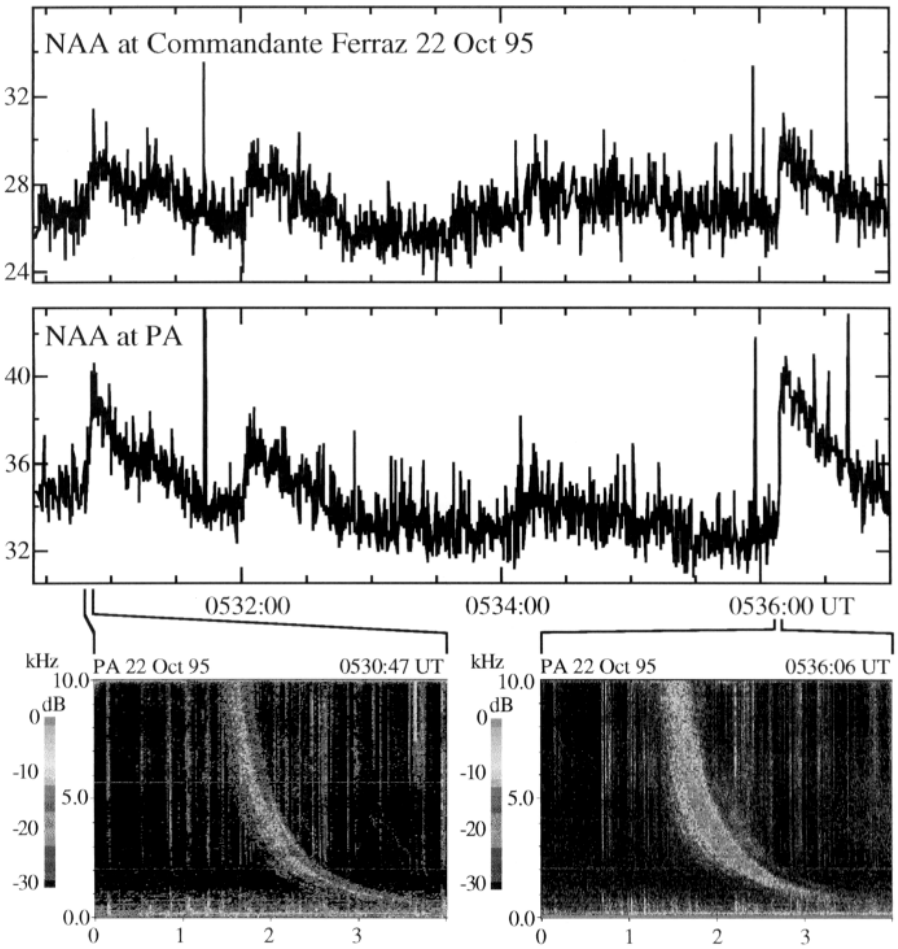

Figure 1. The 24.0-kilohertz (kHz) signal (call letters NAA) from Cutler, Maine, is received at Commandante Ferraz (Brazil) and Palmer Stations in Antarctica (figure 3 is a map showing these stations). Perturbations characteristic of LEP with rapid onset and slow recoveries occur simultaneously at both sites. For the first and last perturbations, broadband recordings from Palmer illustrate the associated ducted whistlers.

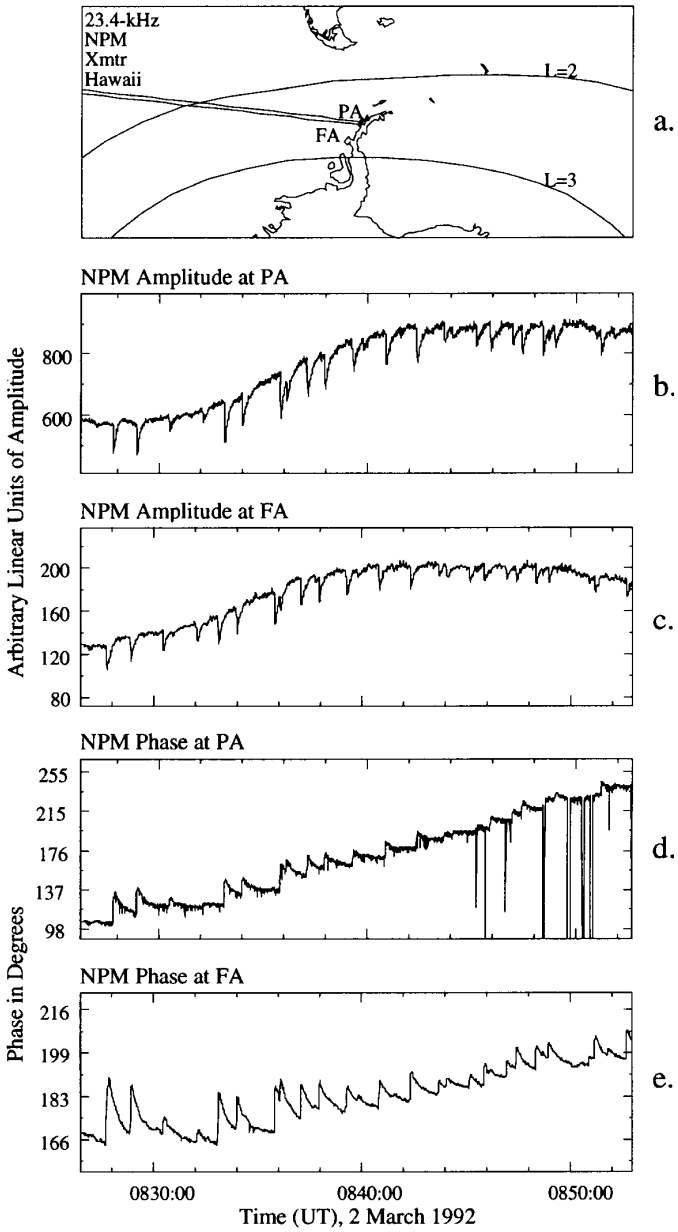

Figure 2. *A.* Map showing the end of the VLF propagation paths from the NPM transmitter to the receivers at Palmer (PA) and Faraday (FA). *B.* NPM signal amplitude showing LEP events recorded at PA during an episode of data on 2 March 1992. This and the three following panels share the same time axis. (UT denotes universal time.) *C.* NPM signal amplitude showing LEP events recorded at FA. *D.* NPM signal phase showing LEP events recorded at PA. *E.* NPM signal phase showing LEP events recorded at FA.

Figure 3. Configuration of proposed VLF measurement sites. The large area covered by three stations will enhance LEP disturbance imaging in the south, conjugate to Northern Hemisphere lightning sources.

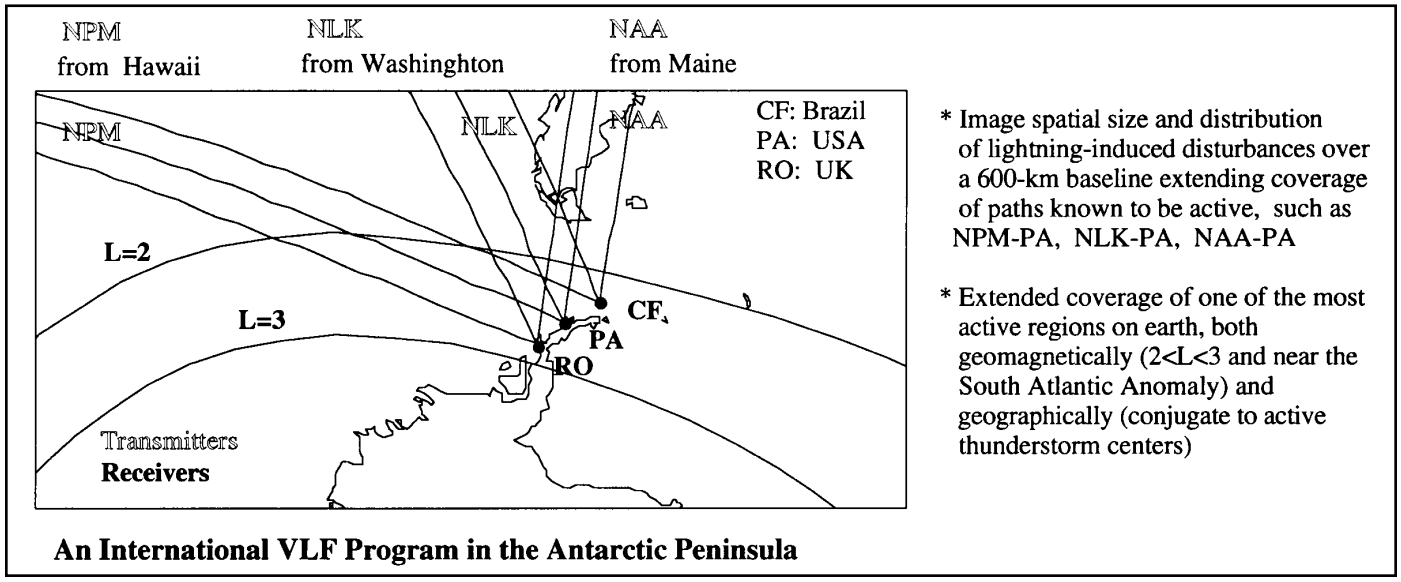

Low-magnitude, long-period magnetic pulsations observed deep in the southern polar cap

V.O. PAPITASHVILI, C.R. CLAUER, *and* S.B. MUSKO, *Space Physics Research Laboratory (SPRL), University of Michigan, Ann Arbor, Michigan 48109*
B.A. BELOV, *Institute of Terrestrial Magnetism, Ionosphere, and Radio Wave Propagation (IZMIRAN), Troitsk, Moscow Region, Russia*
O.A. TROSHICHEV *and* M.G. GUDKOV, *Arctic and Antarctic Research Institute (AARI), St. Petersburg, Russia*

Historically, magnetometer arrays have been the primary tool for studies of the polar ionospheric electric currents, and numerous investigations have been undertaken to clarify the interplanetary magnetic field (IMF) and solar wind control of these current systems (e.g., Clauer and Banks 1986; Papitashvili et al. 1994; and references therein). Supported by our present National Science Foundation award, we have undertaken a cooperative project to deploy and operate digital magnetometers (10-second sampling) at the Russian antarctic stations Vostok and Mirnyy and at two intermediate autonomous sites (geographic and magnetic coordinates are given in the table). The stations complement other data collection in the Antarctic as shown in figure 1.

The stations were deployed during the Russian Antarctic Expedition (RAE) snow traverse from Vostok to Mirnyy in December 1994 and were revisited during the 1995–1996 field season. Unfortunately, the recent RAE snow train was not able to reach Vostok in November 1995; therefore, the RAE made a decision to operate Vostok only through the 1995–1996 summer season (the station was closed on 22 January 1996 and then reopened in December 1996). As a result, the U.S. Antarctic Program provided logistical support to visit Komsomolskaya and Sude from Vostok via the Twin-Otter aircraft in December.

Both autonomous stations appeared to be working, and data were downloaded in the field. Examination of the housekeeping data revealed that both stations had stopped collecting data in September 1995 due to failure of the charging regulators. The Vostok magnetometer system performed successfully through the year, but it was not designed for autonomous operation; so the equipment was removed and shipped to McMurdo for storage at the closure of Vostok. The Mirnyy magnetometer system performed through the 1995–1996 nicely and continues to function. All retrieved data were processed, quality controlled, and can be requested from the SPRL Web site *http://www.sprl.umich.edu/MIST*. The standard WDC-A format 1-minute averages are provided to the AGONET Data Analysis Facility (*http://sunago1.ifsi.fra.cnr.it/adaf.html*).

Already from our newly acquired antarctic data we have discovered a new type of low-magnitude, long-period magnetic pulsations, which appear to be associated only with northward IMF conditions and are observed in only the winter polar cap. Figure 2*A* shows an example of these pulsations observed in the filtered horizontal (H) geomagnetic field component variations on 11 July 1995 (data from the Komsomolskaya station are not available for this day). These pulsations are also seen in the D and Z components. We show here a time interval from 0800 to 1200 universe time (UT) to present the detailed structure of the pulsations; however, they are observed during the entire days of 10–12 July. The northward IMF component measured by the WIND spacecraft was stable during extended period of time. Note that the IMF variations show nothing like these pulsations.

The pulsation period (approximately 15–17 minutes) lies in a lower frequency range of well-known pulsations Pc5, but the magnitude (approximately 3–5 nanoteslas) is much less than the Pc5 magnitude. The pulsations are less pronounced at Sude where we see more high-frequency oscillations; however, the pulsations appear again at Mirnyy. They are also observed at South Pole and automatic geophysical observatory P4 at the same time, but at McMurdo their behavior is similar to what we observe at Sude (Weatherwax personal communication).

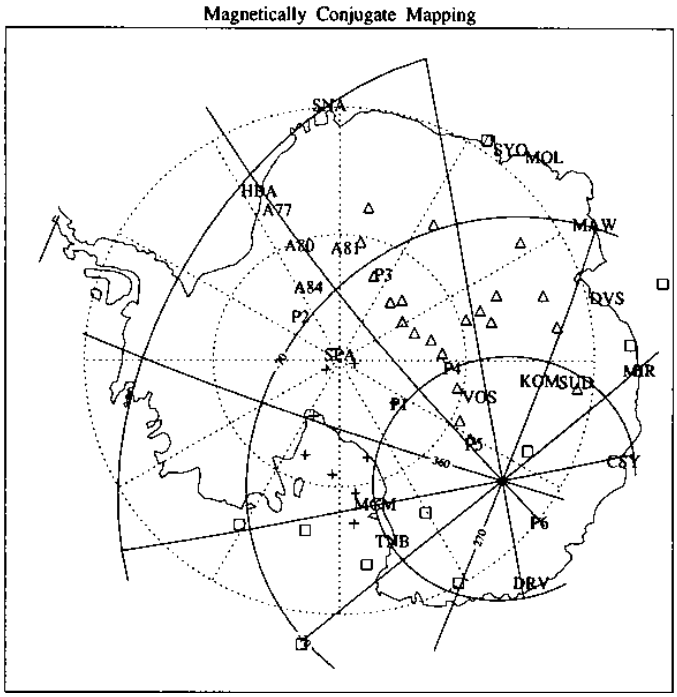

Figure 1. Distribution of the U.S. (designated P#) and British (designated A#) automatic geophysical observatories (AGO) along with Russian stations and other permanent observatories in Antarctica. Magnetic projections of Greenland coastal stations are shown with triangles, Canadian MACCS project stations (with crosses), and northern permanent observatories (with squares).

Figure 2*B* shows power spectra of these pulsations for time interval 0630–1230 UT. As seen, the dominant peak of the approximately 16-minute period appears at all three sites; some longer period waves are also seen. We checked our Greenland magnetometer database, but we were not able to find similar pulsations over magnetically conjugate latitudes in the summer polar cap. We found a few events with similar pulsations, however, at high-latitude Greenland stations which occurred in winter and equinox during northward IMF. This finding suggests an asymmetric response of the polar ionospheres during the northward IMF conditions.

Extending our study, we have found a few other similar pulsation events in the antarctic magnetic data. In each case, the IMF was northward and stable during an extended period

Antarctic magnetometers

	Vostok	Komsomolskaya	Sude	Mirnyy (continued)
International Association of Geomagnetism and Aeronomy code	VOS	KOM	SUD	MIR
Geographic latitude	–78.46	–74.12	–71.30	–66.55
Geographic longitude	106.82	97.50	96.68	93.02
CGM latitude	–83.33	–82.02	–80.93	–77.19
CGM longitude	54.49	90.06	107.03	122.18
Conjugate latitude	77.01	80.05	81.63	80.88
Conjugate longitude	303.40	325.84	343.40	19.75
Magnetic local time noon (UT hours:minutes)	13:03	10:34	9:29	8:25
Data availability	12/01/94–01/22/96	12/22/94–09/22/95	12/26/94–09/09/95	01/03/95–10/22/96

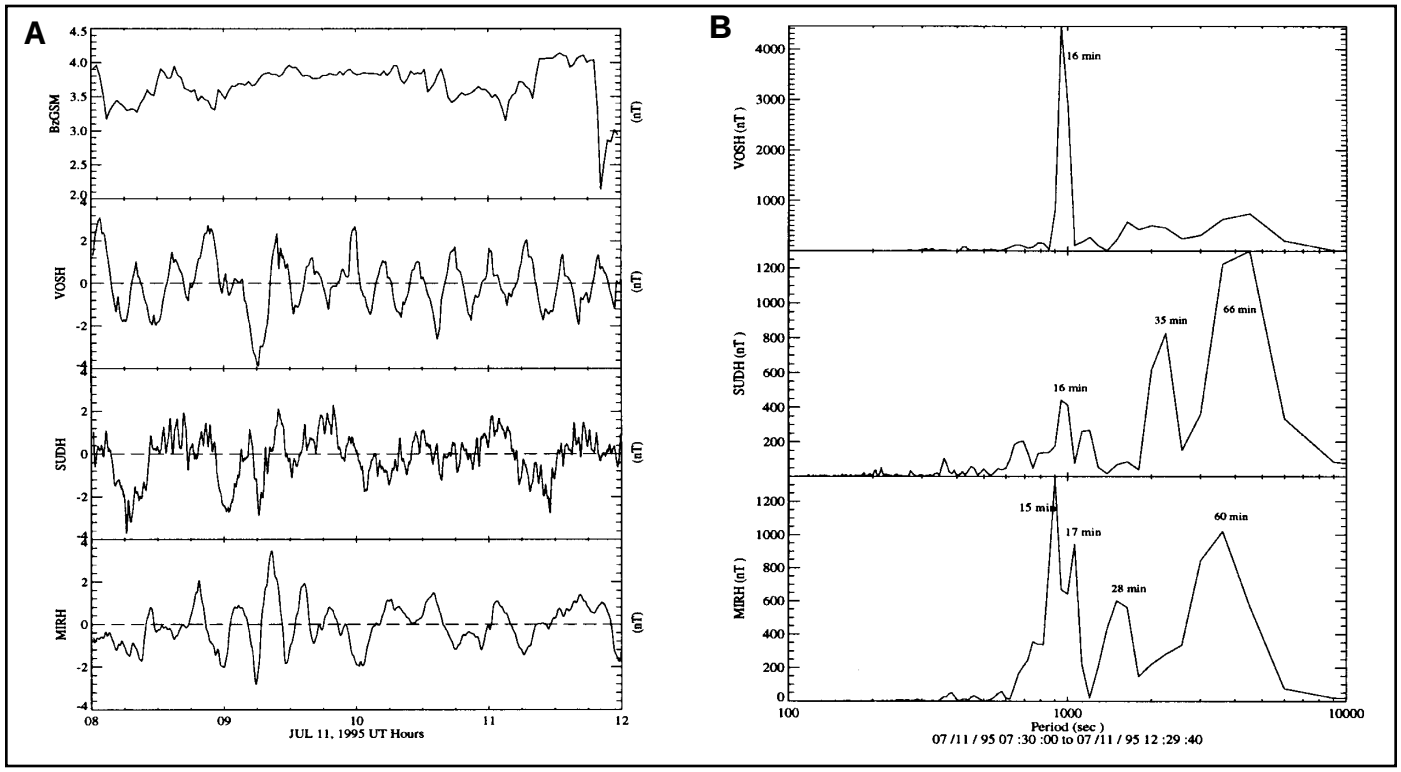

Figure 2. *A.* Shown from the top are the IMF Bz component and the H-component magnetic variations measured at Vostok, Sude, and Mirnyy, respectively, on 11 July 1995. A high-pass filter cutoff period at 2 minutes and a low-pass filter cutoff period at 4 hours were applied to the ground magnetometer data. *B*. Power spectra of the H-component from Vostok, Sude, and Mirnyy for the time interval 0630–1230 UT of 11 July 1995. The peaks around 1000 seconds corresponding to the discovered low-magnitude, long-period (approximately 15–17 minutes) pulsations are evident, as are a number of lower frequency wave components, marked by their approximate period values. (nT denotes nanotesla.)

of time. These events were identified only during austral winter and equinox; no pulsations show up during the austral summer. We plan further study of the discovered low-magnitude magnetic pulsations, particularly to identify the regions over which they are observed using data from other high-latitude stations, and to determine their mapping to the outer magnetosphere using satellite plasma particle data and appropriate models.

This research was supported by National Science Foundation grant OPP 93-18766.

References

Clauer, C.R. and P.M. Banks. 1986. Relationship of the interplanetary electric field to the high latitude ionospheric electric field and currents: Observations and model simulation. *Journal of Geophysical Research*, 91(A6), 6959.

Papitashvili, V.O., B.A. Belov, D.S. Faermark, Ya.I. Feldstein, S.A. Golyshev, L.I. Gromova, and A.E. Levitin. 1994. Electric potential patterns in the northern and southern polar regions parameterized by the interplanetary magnetic field. *Journal of Geophysical Research*, 99(A7), 13251–13262.

Weatherwax, A. 1996. Personal communication.

Large-amplitude hydromagnetic waves on open geomagnetic field lines

A. WOLFE, *New York City Technical College, City University of New York, Brooklyn, New York 11201* and *Bell Laboratories, Lucent Technologies, Murray Hill, New Jersey 07974*

L.J. LANZEROTTI *and* C.G. MACLENNAN, *Bell Laboratories, Lucent Technologies, Murray Hill, New Jersey 07974*

A.T. WEATHERWAX, *Institute for Physical Sciences and Technology, University of Maryland, College Park, Maryland 20742*

The characteristics of large-amplitude Pc5 wave events as measured in the southern polar cap region are reported in this article. These events are found to occur simultaneously over a wide longitudinal separation and, therefore, represent a new discovery at such high geomagnetic latitudes. The initial deployment of several of the automatic geophysical observatories (AGOs) at a geomagnetic latitude of approximately 80°S has enabled these investigations.

Recent Pc5 wave studies at lower latitudes near the nominal nightside auroral zone (approximately 65°) have been reported by Samson et al. (1991, 1992), Ziesolleck and McDiarmid (1994, 1995), and Wolfe et al. (1994, 1995). Samson et al. (1991, 1992) calculated discrete resonant wave frequencies using cavity and waveguide models of the magnetosphere and compared them to published observations. Ziesolleck and McDiarmid (1995), using the CANOPUS magnetometer array in Canada, observed frequencies similar to those of the Samson et al. models. Wolfe et al. (1994, 1995) reported a large-amplitude Pc5 wave event having a frequency near 3 millihertz (mHz) in the southern auroral zone. Higher frequency waves, in the Pc4 (approximately 7–14 mHz) and Pc1–2 bands (220 mHz and 525 mHz) were also found to occur simultaneously with the larger amplitude Pc5 wave.

Wolfe et al. (1994, 1995) suggested that several of these Pc4–5 discrete wave events could be explained by the model of Alpert et al. (1993), which would attribute the fundamental frequency wave to a sudden impulse such as might occur on the dayside magnetosphere. The higher frequency waves in association would then represent the spectral response to an impulse input function in the time domain. Wolfe et al. (1995) extended this study and found large-amplitude Pc5 waves of similar frequency in the conjugate area of the Northern Hemisphere. In summary, these waves were found to occur in both hemispheres, over a longitudinal extent and from auroral zone to near cusp/cleft latitudes.

This study explores a higher latitude region in the southern polar cap. For this purpose, a newly established magnetometer array in Antarctica is used. Two of the six AGOs have recently been located at a geomagnetic latitude of 80° separated by 25° in longitude (AGO-P1 and -P4) under the auspices of the National Science Foundation's polar experiment network for geophysical upper atmosphere investigations (PENGUIN) project. Using data from these locations, together with data from the McMurdo location, we report the occurrence and characteristics of three large-amplitude Pc5 wave events that are found to exist simultaneously over a 75° separation in longitude.

Although the fluxgate magnetometer data are recorded with a 1-second sampling rate, the McMurdo data were decimated to 10-second samples for this initial study. Reported here are analyses of south-north–component data recorded on 12 June 1994. This day is characterized as moderately disturbed geomagnetically, having a geomagnetic index daily sum K_P=30. Concentrated upon in this article are three 1-hour intervals beginning at 1200, 2100, and 2300 universal time (UT). Magnetic local time (MLT) equals UT minus 6.9, 3.7, and 2.0 hours for McMurdo, P1, and P4, respectively. (This interval was a portion of one that has been selected as one of the Scientific Committee on Antarctic Research's AGONET intervals of special interest.)

Figure 1 shows a 1-hour time plot for the 2300 UT wave event. The south-north–component traces from the three stations (McMurdo, P1, P4) show an overall similarity in the

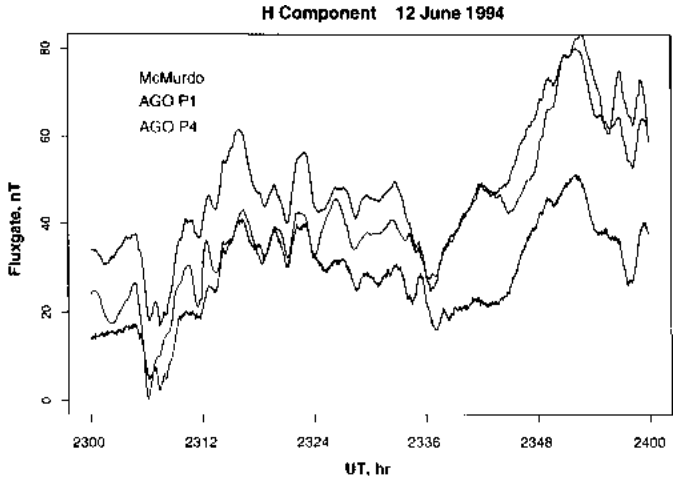

Figure 1. Magnetic field traces [south-north (H) component] from fluxgate magnetometers. From top to bottom at 2300 UT, the traces correspond to AGO-P1, McMurdo (Arrival Heights) and AGO-P4. The hour shown for 12 June 1994 includes a large-amplitude Pc5 wave event between 2310 and 2330 UT.

magnetic variations throughout the hour. For the wavelike variations between about 2310 and 2330 UT, peak-to-peak amplitudes are largest [15 nanoteslas (nT)] at P1, whereas they are nearly equal (10 nT) at P4 and McMurdo (especially between about 2315 to 2324 UT) even though the latter two stations are separated by about 75° in magnetic longitude.

Spectral analyses of the data from the three stations for this hour reveal several discrete frequencies. A number of spectral peaks in the Pc5 range are evident in the spectra shown in figure 2. Prominent ones occur near frequencies of 1.9, 2.8, 4.4, 5.2, and 6.4 mHz. It is especially noteworthy that all three stations record large and comparable amplitudes near the 5.2-mHz peak.

Additional large-amplitude wave events are found at different local times on this day (12 June; data not shown here). For example, an event with frequency approximately 4.5 mHz occurred between 2100 and 2120 UT. At this time, stations P1 and McMurdo have similar, and the largest, amplitudes (15–20 nT) whereas P4 shows a smaller amplitude (10 nT). A third large-amplitude Pc5 wave event (frequency approximately 5 mHz) occurred just after 1200 UT. This latter event occurred during local morning at P1 and P4 whereas the first two events occurred during local afternoon, evening, and early nighttime hours for all stations.

Figure 3 summarizes several characteristics of the three measured wave events that have frequencies near 5 mHz. This summary figure is derived from the hourly power spectra of south-north–component data. It shows the wave power spectral density at the discrete frequencies for the three stations. All events are large-amplitude waves, and the 2300 UT event has comparable amplitudes over the wide azimuthal separation from McMurdo to P4.

As noted above for the event in figure 1 and the spectra in figure 2, additional Pc5 spectral peaks are also found to occur during these times for the other two events. In the intervals of the three wave events reported on here, other discrete dominant frequencies occur near 1.9, 2.5, 2.8, 3.1, 3.6, 3.9, 5.6, and 6.4 mHz, depending upon the specific event.

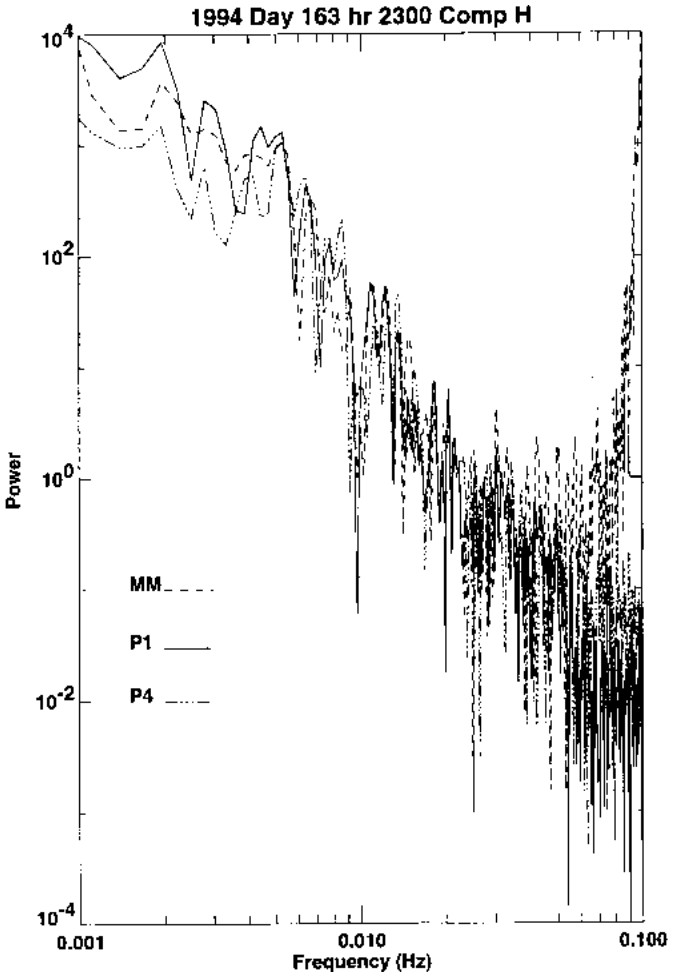

Figure 2. Power spectra of the south-north (H) component data for the time interval shown in figure 1. Several discrete peaks in the Pc5 frequency range are evident simultaneously at the three locations. (MM denotes McMurdo.)

In summary, in the interval analyzed, we find several dominant Pc5 wave frequencies to occur in the southern polar cap region near 80° geomagnetic latitude. Higher frequency waves (5.0, 5.6, and 6.4 mHz) are seen simultaneously at three locations separated by 75° in geomagnetic longitude. Lower frequencies are also found to occur at one or two of the locations (1.9, 2.5, 2.8, 3.1, 3.6, and 3.9 mHz). Auroral latitude studies of Pc5 waves revealed discrete frequencies near 1.3, 1.9, 2.6–2.7, 3.3–3.4 mHz (Ziesolleck and McDiarmid 1994, 1995). The five lowest frequencies reported in this article are nearly equal to the highest frequencies discussed in the above references. Such frequencies have recently been predicted using the cavity, or waveguide, model of the magnetosphere (Samson et al. 1991, 1992). The observations reported here, however, are from higher latitudes and occur near the open-closed magnetic field line boundary.

Evidence for open field lines at the geomagnetic latitude of McMurdo is provided by observations of 30–40-kiloelectronvolt (KeV) electrons that were measured on passes of the

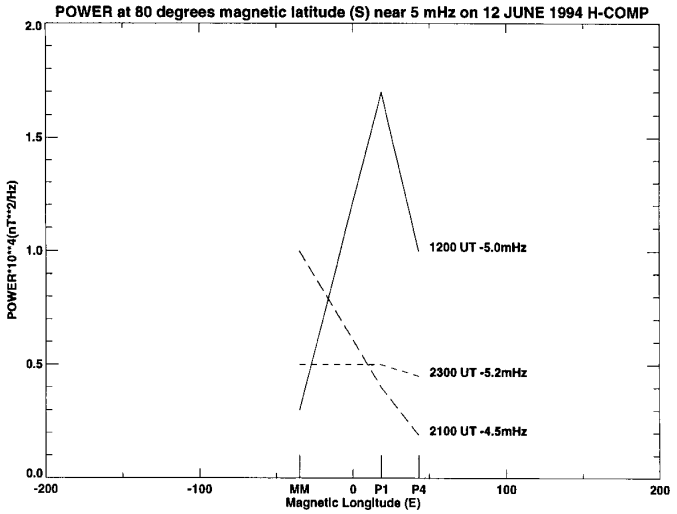

Figure 3. Power spectral density [south-north (H) component] amplitudes at three locations for three wave events having frequencies near 5 mHz. Large-amplitude waves are seen simultaneously over a wide longitudinal separation (75°) in the southern polar cap region.

low-altitude SAMPEX spacecraft across the Antarctic during these intervals (for example, during the interval 2321–2330 UT, the spacecraft passed between McMurdo and P1, about 10° east of McMurdo). The electron fluxes, although high in the auroral zone near latitudes of approximately 69°S, decreased sharply in intensity above approximately 72°S, indicating open field lines above this latitude. Thus, McMurdo was on open field lines during the times of the large-amplitude wave events.

Therefore, it is likely that the considerations of Samson et al. (1991, 1992) are inapplicable to these events. The theoretical treatment by Walker et al. (1993) showed the possibility of the existence of discrete spectra for low-frequency ultra-low-frequency (ULF) waves that are generated in the geomagnetic tail. Such magnetotail oscillations in the Pc5 range could couple onto open field lines to the polar cap ground stations resulting in spectra such as those reported here. This possibility requires further examination to understand the existence and nature of such large-amplitude waves that are observed in the polar cap region over a wide longitudinal separation.

This work was supported in part by a National Science Foundation OPP 89-18689 (PENGUIN) grant to the University of Maryland and subcontracted to Bell Laboratories-Lucent Technologies. We thank T.J. Rosenberg of the University of Maryland and the entire PENGUIN team for their collaboration. We are grateful to G. Mason and J. Mazur of the University of Maryland for the SAMPEX data. We also thank David S. Sayres of Haverford College for his assistance in software development and data processing.

References

Alpert, Y., L.J. Lanzerotti, D.J. Thomson, C.G. Maclennan, A. Wolfe, and R.E. Erlandson. 1993. Hydromagnetic background of the magnetosphere and gyroresonance swinging of a "Giant" Pc2 wave event. *Journal of Geophysical Research*, 98(A5), 7571–7584.

Samson, J.C., R.A. Greenwald, J.M. Ruohoniemi, T.J. Hughes, and D.D. Wallis. 1991. Magnetometer and radar observations of magnetohydrodynamic cavity modes in the Earth's magnetosphere. *Canadian Journal of Physics*, 69, 929.

Samson, J.C., B.G. Harrold, J.M. Ruohoniemi, R.A. Greenwald, and A.D.M. Walker. 1992. Field line resonances associated with MHD waveguides in the magnetosphere. *Geophysical Research Letters*, 19, 441.

Walker, A.D.M., J.M. Ruohoniemi, K.B. Baker, R.A. Greenwald, and J.C. Samson. 1993. Spectral properties of magnetotail oscillations as a source of Pc5 pulsations. *Advances in Space Research*, 13(4), 59–65.

Wolfe, A., L.J. Lanzerotti, C.G. Maclennan, and R.L Arnoldy. 1994. Simultaneous enhancement of Pc1, Pc4, Pc5 hydromagnetic waves at AGO-P2, Antarctica. *Antarctic Journal of the U.S.*, 29(5), 366–369.

Wolfe, A., L.J. Lanzerotti, C.G. Maclennan, and M.J. Engebretson. 1995. Low frequency Pc4–5 hydromagnetic waves at high latitudes in the antarctic and conjugate area. *Antarctic Journal of the U.S.*, 30(5), 364–366.

Ziesolleck, C.W.S., and D.R. McDiarmid. 1994. Auroral latitude Pc5 field line resonances: Quantitized frequencies, spatial characteristics, and diurnal variation. *Journal of Geophysical Research*, 99(A4), 5817–5830.

Ziesolleck, C.W.S., and D.R. McDiarmid. 1995. Statistical survey of auroral latitude Pc5 spectral and polarization characteristics. *Journal of Geophysical Research*, 100(A10), 19299–19312.

Infrared radiation studies of the winter marine antarctic atmosphere

J.L. SIMMONS *and* K. STAMNES, *Geophysical Institute, University of Alaska, Fairbanks, Alaska 99775*
F. MURCRAY *and* X. LIU, *Department of Physics, University of Denver, Denver, Colorado 80208*

Scientists have only a small data set from which to characterize the austral marine radiation environment. Yet, this atmosphere/sea-ice/ocean system is a primary component in the annual global energy budget. The University of Alaska at Fairbanks in collaboration with the University of Denver conducted a small atmospheric radiation campaign in the Ross, Amundsen, and Bellingshausen Seas aboard the R/V *Nathaniel B. Palmer* in August and September 1995. During a variety of meteorological conditions, middle infrared emissions of the winter atmosphere were measured with a Fourier transform infrared (FTIR) spectrometer. The instrument measures zenith radiance from 550 inverse centimeters (cm^{-1}) to 1,650 cm^{-1} [18 to 6 microns (μm)] with 1-cm^{-1} resolution. This wavelength interval is particularly useful because it contains not only much of the blackbody emission for the cold polar atmosphere but also major emission bands for such trace gases as carbon dioxide, ozone, and water vapor.

The instrument was mounted in a portable, insulated house on the back deck of the *Palmer*. Each 15-minute measurement sequence viewed the zenith sky emission and two calibration blackbodies. Weather permitting, the instrument was operational several hours per day along the cruise track shown in figure 1. Radiosondes were also launched from the ship, providing vertical profiles of atmospheric pressure, temperature, and relative humidity to accompany the radiometric measurements. The upper deck and mast of the ship were equipped with a standard meteorological equipment package and a ground-based ultraviolet radiometer (GUV).

Longwave radiation in the clear atmosphere

Figure 2 is an example of clear-sky emission in the Ross Sea. Carbon dioxide (667 cm^{-1}), ozone (1,042 cm^{-1}), and water vapor (1,595 cm^{-1}) are major contributors to the infrared radiance observed at the sea-ice surface (Lenoble 1993). The region between the large carbon dioxide band and the water vapor band is known as an "atmospheric window" (770–1,250 cm^{-1}, 8–13 μm). It is relatively transparent but still contains ozone emission, water-vapor continuum emission, and weak lines of other trace gases. A second window (360–625 cm^{-1}), partially captured by the FTIR, is often found in the polar regions where water vapor is minimal, as seen in figure 2.

Longwave radiation in a cloudy atmosphere

Many cloud types, ranging from thick, low stratus to altocumulus rolls, were observed along our cruise track. Atmospheric emission received at the surface is greatly increased with the presence of clouds, which close the atmospheric windows. Two cloudy emission spectra, recorded in the Bellingshausen Sea, are shown in figure 3. Curve A represents emission from a developing stratus cloud deck.

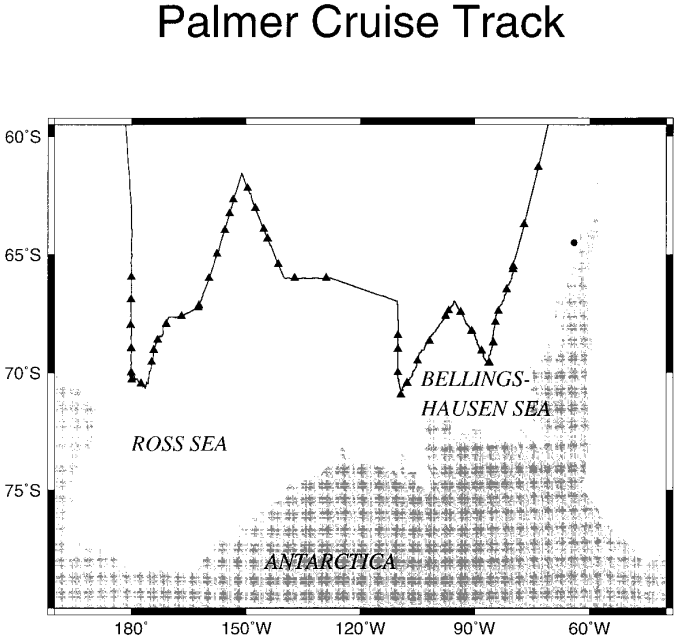

Figure 1. Map of the cruise track of the R/V *Nathaniel B. Palmer* in August and September 1995. Each triangle is the site of a radiosonde launch and the circle marks the location of Palmer Station.

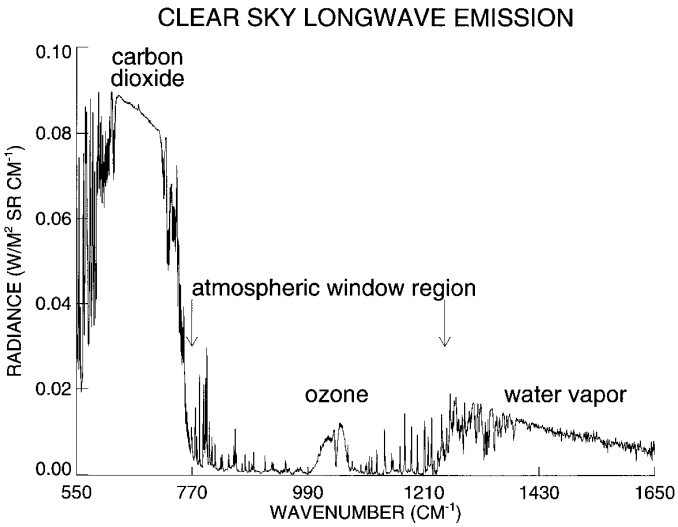

Figure 2. Infrared, zenith emission spectrum of a clear atmosphere, Ross Sea (67°56'S 170°56'W), 15 August, 23:55 Greenwich mean time, measured by the FTIR. The near surface temperature was approximately –16°C. (W/M^2 SR CM^{-1} denotes watts per meter squared per inverse centimeter.)

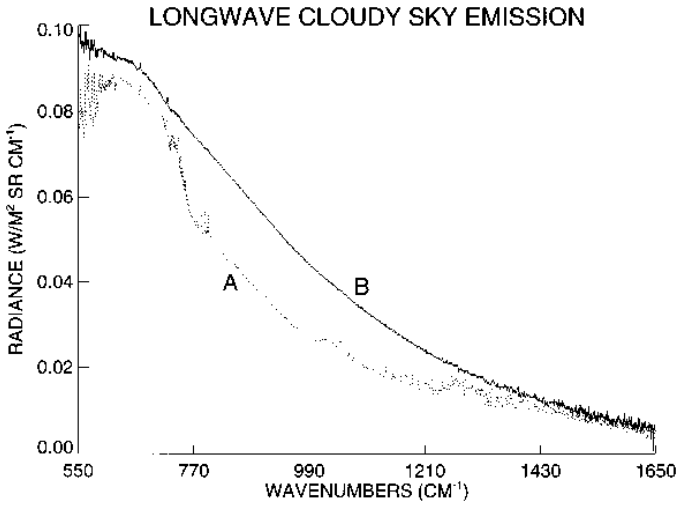

Figure 3. Infrared, zenith emission spectra under two cloudy-sky cases. Curve A was recorded in the Bellingshausen Sea (68°48'S 90°38'W) 5 September under a developing stratus cloud. Curve B was recorded in the same location 1.5 hours later under a low, precipitating cloud. The near-surface temperature also increased from –15.5°C to –12.2°C during this period. (W/M^2 SR CM^{-1} denotes watts per meter squared per inverse centimeter.)

Although many of the trace-gas emission lines in the 8–13-µm atmospheric window are now obscured, the ozone emission feature is still present. Future radiative transfer calculations will be used to determine if this contribution comes from stratospheric ozone above the cloud or tropospheric ozone below the cloud base (Lubin and Gautier 1992).

Curve B, observed 1.5 hours after curve A in the same location, is emission from a snowing cloud. The snow cloud radiates nearly like a blackbody and doubles the surface radiance measured under a clear sky. These two spectra highlight the dramatic effect of clouds on longwave surface radiation. Clouds must be characterized correctly in modeling exercises in order to obtain accurate values of surface radiance. As an example, models often treat clouds as black or gray emitters. Preliminary analysis of our data and the observations of Lubin (1994) at Palmer Station suggest that precipitating maritime antarctic clouds have emissivities very close to unity, but that cloud types, such as the stratus shown in curve A, figure 3, have emissivities less than unity.

Future work

Currently, we are performing error analysis on the spectra. When this task is complete, we will begin a cloud radiative properties study, which involves determining cloud emissivity and optical depth from the observed emission spectra and radiative transfer computations. Further, we hope to extract cloud microphysical properties following the methods developed by Lubin and other collaborating universities. In addition to quantifying these cloud parameters, we will perform trace-gas emission and abundance studies of the late winter, marine atmosphere.

Small field campaigns and cooperative investigations between many universities and geophysical disciplines will benefit the advancement of antarctic science. We hope our FTIR and supplementary data will complement radiometric measurements made in the interior plateau at Amundsen–Scott South Pole Station (Walden 1995) and the coastal Palmer Station (Lubin 1994) and assist in quantifying the longwave radiation budget across the entire antarctic region.

We would like to thank Martin Jeffries, sea-ice researcher at the University of Alaska at Fairbanks, for inviting us to participate in his dedicated cruise on the R/V *Nathaniel Palmer*. We would like to thank the Atmospheric Technology Division at the National Center for Atmospheric Research for providing us with the radiosonde system and support and the Antarctic Support technicians for their assistance during the cruise.

This work was supported by National Science Foundation grant OPP 95-23260 to the University of Alaska at Fairbanks.

References

Lenoble, J. 1993. *Atmospheric radiative transfer.* Hampton, Virginia: A. Deepak.

Lubin, D. 1994. Infrared radiative properties of the maritime antarctic atmosphere. *Journal of Climate,* 7, 121–140.

Lubin, D., and C. Gautier. 1992. Fourier Transform Infrared spectroradiometer measurements of atmospheric longwave emission over Palmer Station, spring 1991. *Antarctic Journal of the U.S.*, 27(5), 276–278.

Walden, V.P. 1995. The downward longwave radiation spectrum over the antarctic plateau. (Doctoral thesis, University of Washington, Seattle, Washington.)